2013-01-30

Ischemia-Reperfusion Arrhythmias and Intercellular Coupling in Diabetic and Ischemic-Preconditioned Rat Heart

Randall, Alyssa

UNIVERSITY OF CALGARY

Ischemia-Reperfusion Arrhythmias and Intercellular Coupling in Diabetic and Ischemic-Preconditioned Rat Heart

by

Alyssa Randall

A THESIS

SUBMITTED TO THE FACULTY OF GRADUATE STUDIES

IN PARTIAL FULFILMENT OF THE REQUIREMENTS FOR THE

DEGREE OF MASTER OF SCIENCE

GRADUATE PROGRAM IN BIOMEDICAL ENGINEERING

CALGARY, ALBERTA

JANUARY 2013

Abstract

Diabetes and Ischemic Preconditioning (IPC) have been shown in literature to have similar metabolic and microscopic effects on intercellular coupling, conduction reserve, and the response to ischemia-reperfusion in ventricular tissue. Both diabetes and IPC cause reduced intercellular coupling; reduced conduction reserve; and provide cardio-protection to ischemia/reperfusion. To determine the whole heart similarities between IPC and diabetes both electrocardiograph (ECG) and optical mapping data was evaluated. Diabetes displayed different time dependent responses to ischemia/reperfusion from IPC and healthy animals; diabetic animals slow heart rate significantly compared to IPC and control animals during ischemia, while IPC slows conduction velocity. During pacing, IPC and diabetic animals showed similar slowing of conduction velocity though only diabetic animals showed significant slowing in response to reduced cellular excitability. This work suggests IPC and diabetes do not use the same mechanisms to provide cardio-protective effects.

For Charles, who brings me joy each day.

Acknowledgements

My great thanks to my advisory Dr Anders Nygren; without his guidance, support and patience this work would not have been possible.

Additional thanks to Dr.Yakhin Shimoni for training me, and helping me with my early experiments. Shahir Mishriki for his long hours of data collection and preliminary data analysis which was critical to this work. Parisa Rahnema, who's raw data saved countless hours of data collection and saved many animal lives.

Contents

Tables

Figures

Chapter 1 Background

1.0 Introduction

Diabetes is a growing epidemic in first world countries. The number of adults affected by diabetes is expected to grow from 135 million in 1995 to over 300 million by 2025 [1]. Diabetes increases the risks of stroke, limb loss and myocardial infarctions [2] and has an array of implications for a patient's overall health.

One diabetes-related health concern is cardiovascular complications including diabetic cardiomyopathy. Diabetes-induced cardiac dysfunction includes electrical abnormalities. Similar abnormalities have been seen in ischemic preconditioned hearts.

Both IPC and diabetes are causes of arrhythmias/fibrillation. IPC and diabetes have extensively been compared on a microscopic level due to their metabolic similarieties and response it ischemia reperfusion. The purpose of the proposed research is to compare ischemic preconditioning (IPC) to diabetes with respect to arrhythmia protection on a whole heart level, to determine if the metabolic similarities result in a similar cardio-protective mechanism.

1.0 Objectives and Hypothesis

There are striking similarities between the effects of diabetes and IPC on intercellular coupling, conduction reserve, and response to ischemia-reperfusion in ventricular tissue:

1) Both diabetes and IPC cause reduced intercellular coupling and reduced conduction reserve. [3] [4]

2) In both diabetes and IPC, this reduced intercellular coupling has been linked to increased phosphorylation of Connexin-43 (Connexin 43, the main Connexin responsible for forming intercellular electrical connections in the ventricle of the heart) by protein kinase Cε (PKCε), suggesting a common underlying mechanism. [3] [4]
3) In both diabetes and IPC, activity of calcium-independent phospholipase A2 (iPLA2) is known to be increased (again, suggesting a common mechanism). [5] [6]
4) Both diabetes and IPC have been shown to reduce the incidence of ischemia-reperfusion arrhythmias. [7] [8]

Our lab has demonstrated that intercellular coupling is compromised in hearts of rats made diabetic using streptozotocin (STZ) treatment [4]. This moderate uncoupling is manifested functionally as an increased sensitivity of the cardiac conduction velocity (reduced conduction reserve) to influences that slow conduction (reduced excitability, further uncoupling). Our lab has also demonstrated that conduction velocity in the STZ-diabetic heart is more sensitive to ischemia than that of healthy control hearts. This response was shown to be at least in part related to the activation of iPLA2 in the diabetic hearts.

IPC has been studied extensively in the literature. The fundamental observation, as it relates to this project, is that a brief (few minutes) period of ischemia, followed by reperfusion, significantly reduces the incidence of severe arrhythmias during a subsequent longer-lasting period of ischemia [9]. Recent literature has connected this response to a moderate decrease in intercellular coupling that may be similar to that observed in STZ-diabetic hearts [10].

To compare IPC and diabetes on a macroscopic, whole heart level the project will test the following hypotheses:

1) STZ hearts and healthy control hearts subjected to IPC have similar frequency of ischemia-reperfusion arrhythmias.

2) STZ hearts and healthy control hearts subjected to IPC have similar reductions of conduction reserve.

3) IPC does not further reduce conduction reserve or frequency of ischemia-reperfusion arrhythmias in STZ hearts.

1.1 The Cardiovascular System

The cardiac system consists of the heart and the circulatory system (Figure 1).The right side of the heart pumps blood to the lungs where carbon dioxide leaves the blood and oxygen enters. The blood is then moved to the left side of the heart, completing the pulmonary circuit. Once in the left side it is pumped throughout the body. Once the blood leaves the heart it enters the arteries, flows into the arterioles and finally the capillary beds. Once in the capillary bed, nutrients and oxygen leave the circulatory system and enter the tissue. This is where carbon dioxide and waste products leave the tissue and enter the circulatory system. From the capillaries, blood enters the venules and from there the veins, which connect back to the right side of the heart, completing the systemic circuit. Arteries and veins are the largest of the blood transport structures followed by arterioles and venules, with the capillaries being the smallest.

Organs such as the kidneys and liver are responsible for removing waste from the blood, similar to how the lungs oxygenate the blood while removing carbon dioxide. [11]

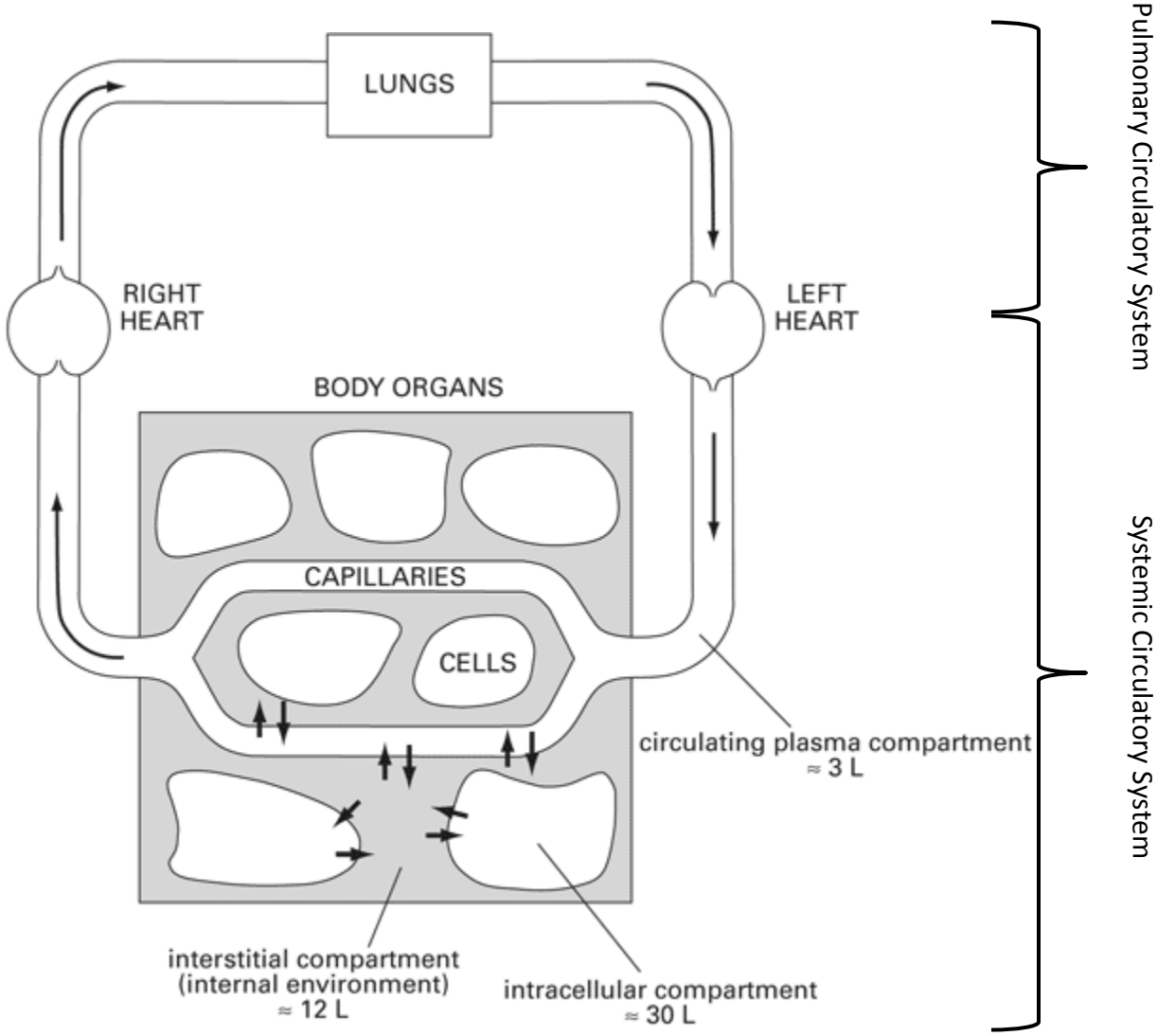

Figure 1 Major body fluid compartments with average volumes indicated for a 70-kg human. Total body water is about 60% of body weight. Division into systemic and pulmonary cardiac systems. Adapted from Mohrman and Heller (2006) **[11]**.

For adults at rest, the heart pumps about 3L of blood continuously around the body at a rate of approximately 5L/minute; this rate is known as the cardiac output of the heart. Cardiac output is

determined by the volume of blood pushed out of the heart (ejection volume) with each heart beat and the number of heart beats per minute. During exercise both ejection volume and heart rate increase to result in a cardiac output of up to 25L/min. [11]

There are three layers of tissue in the heart. Beginning with the innermost layer and moving outward, they arethe endocardium, which is the innermost layer of tissue and composed of endothelial tissue that lines blood vessels the myocardium , a striated muscle and is responsible for the heart's contractions, and finally the epicardium, the outmost layer of heart tissue. The heart is encased in a protective sack called the pericardium which provides low friction movement during contraction.

The heart cycle begins with diastole, which is when the heart is at rest (Figure **2**: A). The blood pressure is at its lowest and blood is filling the atria and ventricles. Near the end of the diastolic phase the atriums contract pushing their blood into the ventricles and the valve that separates the two chambers closes (the mitral valve in the left heart). The ventricles begin to contract, which starts the systolic phase (Figure **2**: B). Initially during contraction the aortic valve that leads to the circulatory system is closed, resulting in ventricle pressure increasing without a change in blood volume (isovolumetric contraction, Figure **2**: C). Once the ventricles reach a threshold pressure, (also known as the diastolic pressure which is typically 60 to100 mmHg in healthy adults) the aortic valve opens and blood is pushed out of the ventricles into the circulatory system. The maximum pressure generated by this push is referred to assystolic pressure (90 to 140 mmHg in healthy adults). Once the ventricle pressure drops below the diastolic pressure the tricuspid valve closes, though the ventricle continues to relax (isovolumetric relaxation, Figure **2**:

D). This continues until the ventricle reaches the same pressure as the atrium at which time the mitral valve opens and the process repeats.

The "Lub Dub" (Figure **2**, S1 and S2 respectfully) sound generated by the beating heart is the result of the valves of the heart closing. "Lub" is generated when the mitral valve closes, at the end of the diastolic phase while "Dub" is generated near the end of the systolic phase when the tricuspid valve closes. Additional heart sounds can sometimes be heard as the result of misaligned closing left and right heart valves or due to valve damage.

1.2 Electrical Conduction Pathways of the Heart:

Heart contractions are controlled by bioelectricity. The heart has a specific electrical system in which a small group of cells initiate an entire heart contraction. These cells make up the sinoatrial node (SA node) and are often referred to as the "pacemaker cells". The SA node spontaneously generates an electrical signal at a rate of 60 to 100 beats per minute. The electrical signal generated by these cells sweeps across the left and right atrium, causing them to contract (Figure **2**). As the atrial muscles complete their contraction the AV node fires and electrical signal transmission speed is slowed. The Purkinje fibers are stimulated after the atria are done contracting and the signal is passed into the left and right ventricle causing ventricle contraction. The signal slowing between the atriums and ventricles allows for full atrium contraction, pushing all the blood into the ventricles, before the ventricle contraction sends the blood into circulation.

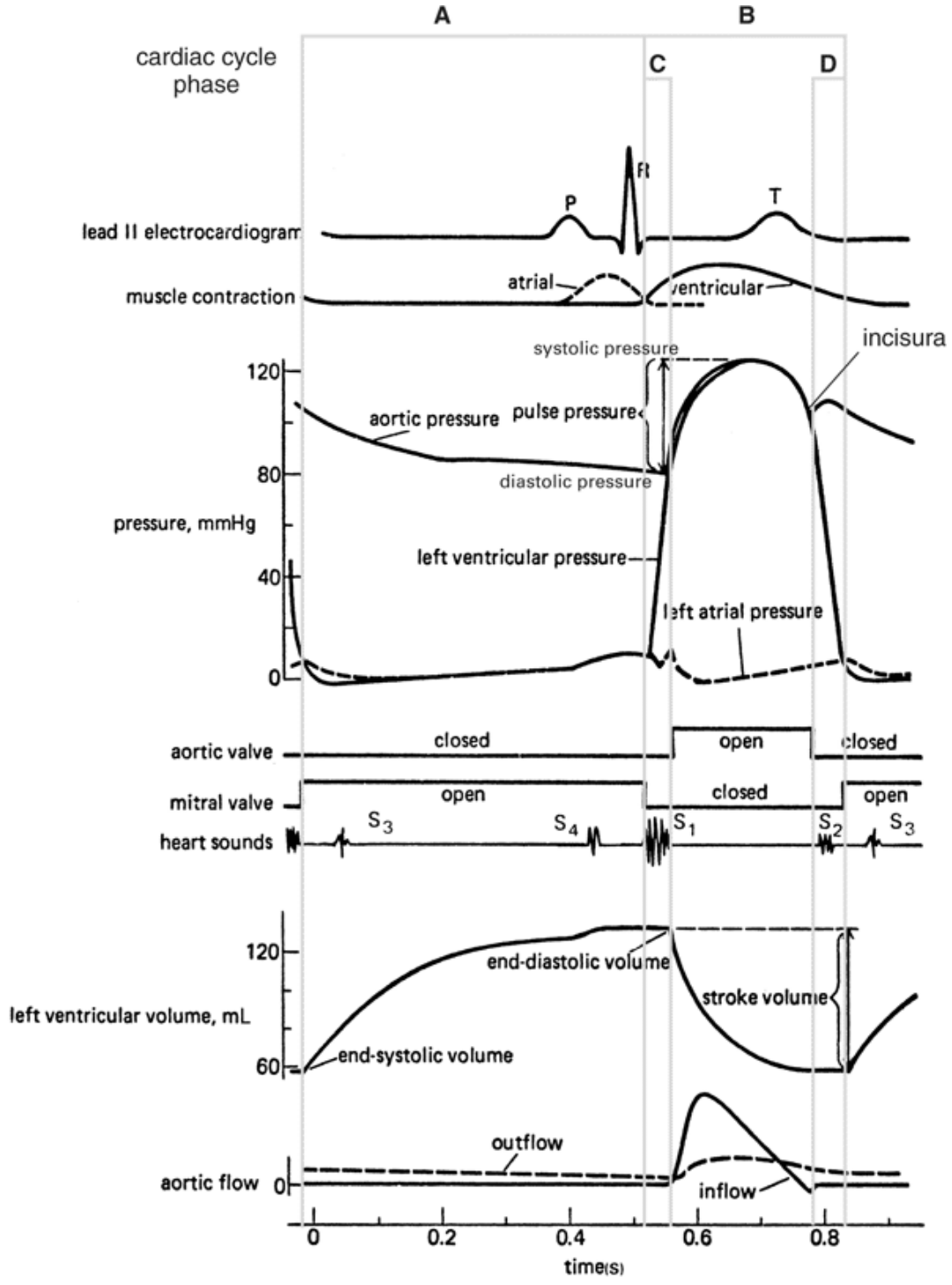

Figure 2 Cardiac cycle - Left heart cycle phases: A diastole; B systole; C isovolumetric contraction; and D isovolumetric relaxation. **[11]**

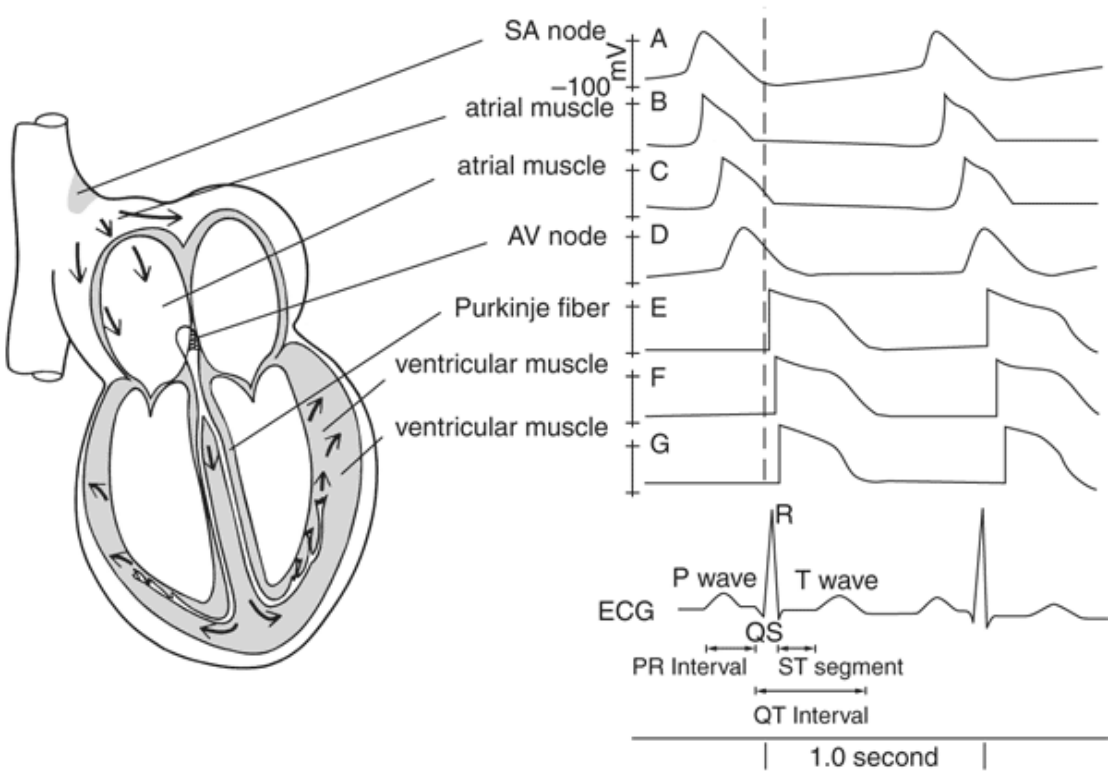

Figure 3 Electrical activity of the heart: single-cell voltage recordings (traces A to G) and lead II electrocardiogram. **[11]**

The electrical signals which induce the contraction of the heart are recorded using an Electrocardiograph (ECG). Electrodes are placed on the skin in a triangle formation around the heart, with two electrodes located at the tops of the right and left ventricles and a third electrode below the apex of the heart. The ECG is recorded via a differential signal between two of three electrical channels, generating three channels know as Lead I, II, and III. The most common ECG channel used is the Lead II channel resulting from a differential between the inferior apex channel and the superior right channel (Figure 3). [11]

A normal Lead II ECG trace consists of five easily recognizable wave forms. These waveforms are known as the P, Q, R, S and T waveforms (shown in Figure 3). The P wave is attributed to the depolarization and repolarization of the atriums. The QRS complex is attributed to the ventricular depolarization and should take less than 120 msec; while the time between the P and R waves should be no more than 200 msec (indicating proper conduction delay between atria and ventricular depolarization). The T wave represents the ventricle tissue repolarization with a healthy QT interval of no more than half the full ECG interval (the R-R interval). [11].

The rat has a similar ECG to that of a human, with a higher heart rate and therefore shorter interval times. For example, in a healthy adult Wistar rat the heart rate is approximately 344 beats per minute with a PR interval of 65msecs and a QRS interval of 23 msec [12].

1.3 Electrophysiology

The electrical properties of the heart are generated by electrochemical differences across the cell membranes of individual cells. Na^+, K^+ and Ca^{2+} ions are all key to the electrochemical properties of a single cell. The cell membrane has a number of ion channels and rectifying ion channels which will open or close depending on the voltage gradient across the cell membrane. Changes in the charges of neighboring cells may induce excitation of the cell by raising its membrane potential above the threshold.

At "rest" the inside of a cell is close to the equilibrium potential of K^+ (-85 mV). This resting value varies marginally between cell types and is always referred to as the resting membrane

potential.

A neighboring positive charge changes the opened and closed states of the ion channels in the cell. The cell depolarizes quickly as the Na^+ channels open. This increases the overall charge of the cell as Na^+ ions rush into the cytoplasm. The cell's charge quickly approaches the Na^+ equilibrium of +60mV. This stage is referred to as the depolarization of the cell.

As the cell rapidly approaches +60mV the Na^+ ion channels begin to close and transient outward K^+ channels begin to open. Thus the influx of Na^+ ions stop and the efflux of K^+ ions begin, lowering the cell's electrical potential. This is followed by a plateau caused by the Ca^{2+} (L – Type) channels where the inward flux of Ca^{2+} balances the charges leaving the cell through the K^+ current. Once the L-Type Ca^{2+} channels close the K^+ channel conductance increases and more K^+ channels are activated. This resumes the repolarization of the cell, which continues until the cell approaches the resting potential.

The K^+, $Ca2^+$ and Na+ ions are slowly returned to their original relative concentrations within and outside the cell through ion leak channels and pumps like the Na^+/K^+ pump, which pushes 3 Na^+ ions out of the cell while bringing in 2 K^+ ions. The cell has a refractory period where it cannot be reactivated because the Na^+channels have to recover from inactivation (even though the cell has returned to its resting potential). This depolarization and repolarization referred to as an action potential. Once the tissue has returned to its resting ion state it may be reactivated.

As one cell depolarizes and becomes positively charged it affects the resting potential of the neighboring cells. If the effect is great enough this will induce depolarization. This effect allows an action potential to travel across an entire tissue after a single region depolarizes. Due to the refractory period of the tissue, cells that were recently activated cannot be reactivated, thus the action potential can only travel forward.

1.6 Gap Junctions

Gap junctions are groupings of transmembrane channels which connect the intracellular compartments of nearby cells. This cell to cell connection results in a low resistance transmission of electrical stimulation, resulting in synchronous contractions. Figure 4 shows the structure of gap junctions.

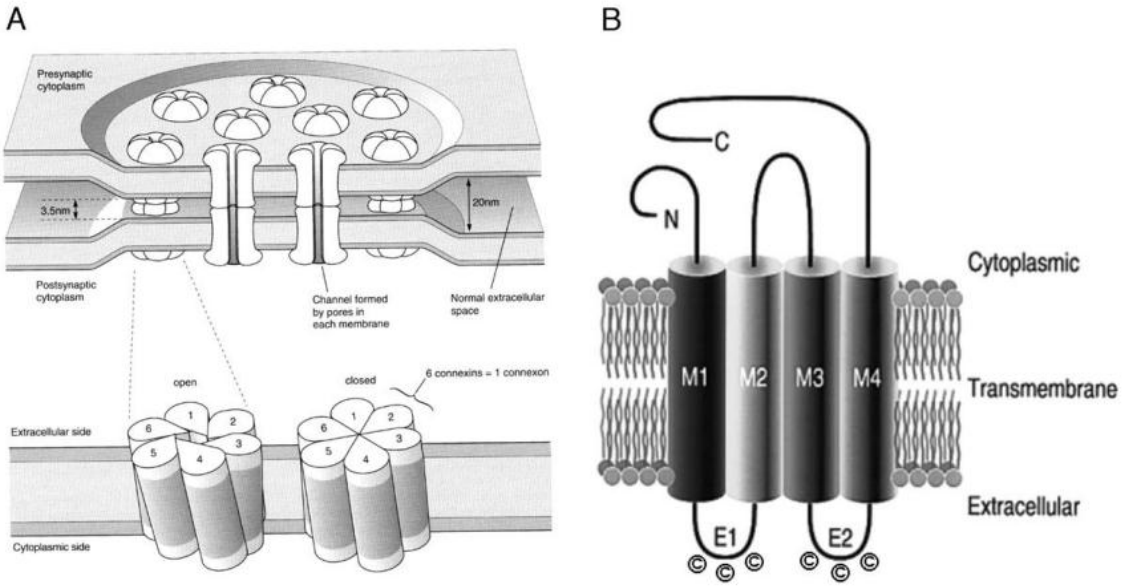

Figure 4 (A) *Schematic drawing of gap junction channels.* Each apposed cell contributes a hemi-channel to the complete gap junction channel. Each hemichannel is formed by six protein subunits, called Connexins. Six Connexin subunits of the hemi-channel may coordinately change

configuration to open and close the hemi-channel. Closure is achieved by Connexin subunits sliding against each other and tilting at one end, thus rotating at the base in a clockwise direction. The darker shading indicates the portion of the Connexin embedded in the membrane. (B) *Topological model of a Connexin*. The cylinders represent transmembrane domains (M1– M4). The loops between the first and the second, as well as the third and fourth transmembrane domains, are predicted to be extracellular (E1 and E2, respectively), each with three conserved cysteine residues. [13]

Gap junctions are mainly located at the end to end intercellular connection of the "rod-shaped" cells as (shown in Figure **5**) for healthy tissue [4]. Each channel is constructed from two hemichannels where each hemichannel is composed of proteins called Connexin [13]. Each hemichannel is made of a single or multiple Connexin types. Within the myocardium Connexin 40, 43 and 45 are the most common isoforms. Each isoform populates a specific region; however, Connexin 43 is the most common within the heart, especially within the ventricular myocardium. Connexin 43 is rare/absent in some areas of the conduction system where Connexin 40 and 45 are the major isoforms [14]

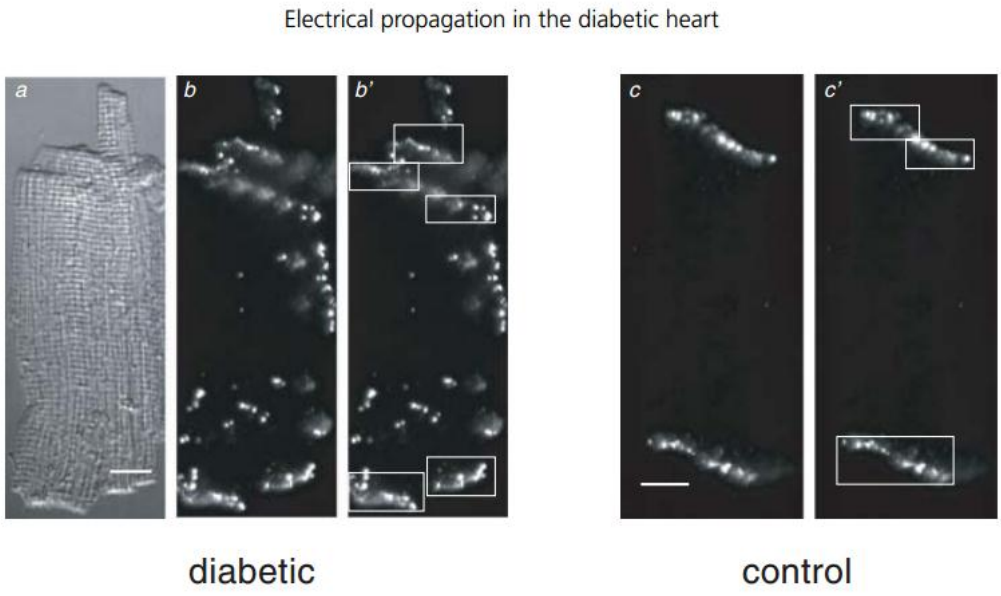

Figure 5 Analysis of lateralization of Connexin 43

Panels a–b, differential interference contrast (a) and immunofluorescence (b and b) images of an isolated ventricular myocyte from an STZ-diabetic rat heart labelled with anti-Connexin 43. Panels c and c: immunofluorescence images of an isolated ventricular myocyte from a non-diabetic (control) rat heart labelled with anti-Connexin 43. White rectangles in b and c surround the intercalated discs. Scale bars in panels a and c represent 10 μm. **[4]**

Each Connexin isoform has its own electrical conductance properties. Therefore the type and quantity of each type of Connexin is a key determinant in the channel conductance as well as the electrophysiological properties of the gap junctions [13]. Higher incidence of ventricular fibrillation has been related to a decrease in Connexin 43 immunopositive gap junctions [15]

Reduced membrane excitability often occurs alongside coupling anisotropy and impairment. The reduction in cell membrane excitability is counteracted by decreased coupling, causing mixed results. Therefore, in pathological conditions, the conflicting effects are of considerable

importance. Reduced cellular coupling decreases the electrical sink required to be overcome for cell excitation, therefore compensating for decreased membrane excitability with regards to propagation, arrhythmogentity and refractoriness [16].

1.4 Cardiac Abnormalities

The ECG is extremely useful as a noninvasive tool to determine cardio-electric health problems. Examples of supraventricular arrhythmias are shown in Figure **6**. These arrhythmias are caused by issues before ventricle depolarization. Supraventricular tachycardia is when the SA node is overridden by a higher rate of depolarization of the atria, causing rapid contractions of the whole heart. First through third degree block occurs when signal transmission from the atrium to the ventricles through the AV node are slowed, resulting in a longer PR interval or the signal only being carried through part of the time. Finally, atrial fibrillation occurs when there is no synchrony with atrium contractions. This results in random activation of atrial cells and the AV node inducing ventricle contraction at irregular intervals.

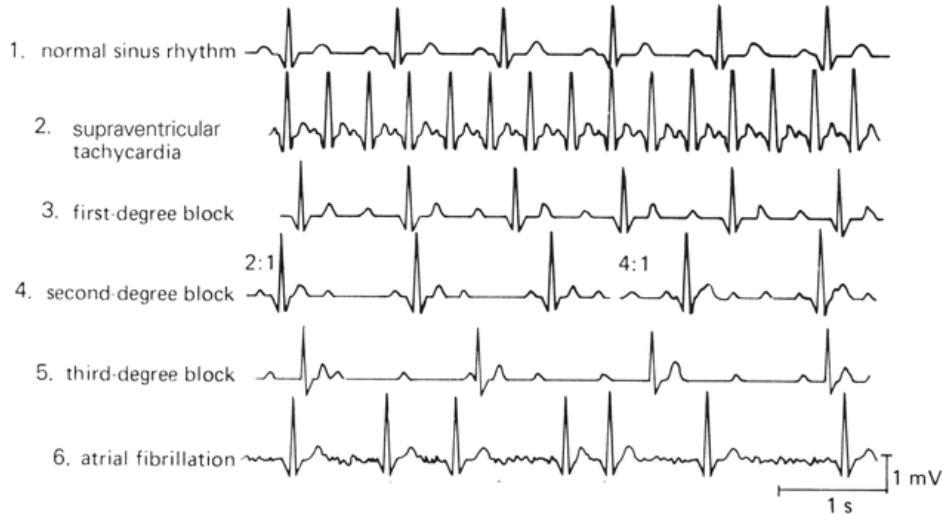

Figure 6 Examples of supraventricular arrhythmias **[11]**

Figure **7** shows common ventricular abnormalities. Bundle branch blocks can occur due to myocardial infarction (tissue death) in the Purkinje system. As a result, part of the conduction pathway is no longer capable of transporting the electrical signal and longer time is required for the ventricles to contract (lengthening the QRS complex). Premature ventricular beats occur when the ventricle depolarizes before the signal from the atrium. This is often followed by a missed beat due the lengthy repolarization time of the ventricle tissue.

Ventricle tachycardia occurs when a group of cells become excitable at a high rate overriding the SA node's pace. The result is rapid contractions of the ventricles. Prolonged QT intervals often result from ion channel abnormalities and can result in tachycardia or fibrillation of the tissue. Finally, ventricular fibrillation is when an electrical signal does not die out, but continues to travel through the ventricle tissue causing random tissue activation. This results in the tissue being unable to properly contract.

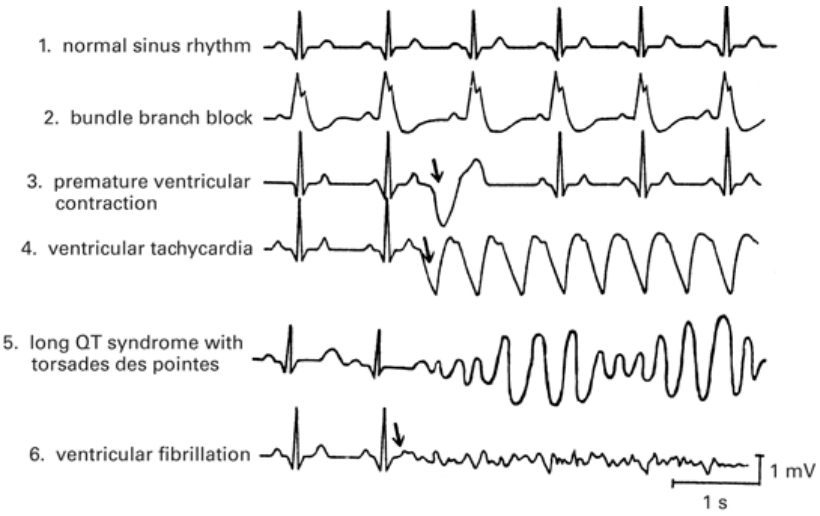

Figure 7 Examples of Ventricular Arrhythmias **[11]**

1.5 Fibrillation

Fibrillation results from re-entry of a singular electrical stimulation into tissue already activated by the electrical signal (normally tissue is activated once per electrical signal). When an electrical signal propagates from the SA node through the heart there is a long refractory period (in healthy tissue). As a result, the "wave front" or electrical signal eventually hits a region of tissue that is still in its refractory period and the signal dies out [17]. If the conduction velocity (the speed of the electrical signal) of the tissue is slowed then previously activated tissue can be reactivated, and the signal continues instead of dying out (sustained conduction). Also, if there is a greater heterogeneity of conduction velocity then the excitation wave front may interact with the repolarizing phase causing a conduction block, effectively creating a dead zone. Should a conduction block occur the electrical signal may rotate around the block, returning to the original site of tissue with enough time having lapsed for propagation to continue [18].

The safety factor of impulse propagation is the margin with which an electrical signal (action potential) propagates with respect to the minimum requirements for sustained conduction (fibrillation) [19]. The safety factor has been shown to be affected by a number of electrophysiological characteristics including intercellular coupling and cell excitation. Cells have excess gap junction conductance to ensure that a safe impulse propagation factor is maintained: this is referred to as the conduction reserve [20].

Figure 8 shows the effect of gap junction coupling on conduction velocity. In the plateau region (control) a reduction in gap junction coupling has little effect on conduction velocity. Within healthy tissue a reduction of 43% of CConnexin expression elicits a minor reduction in conduction velocity (Thomas, Kucera et al, 2003). The less the initial coupling, the greater the effects of moderate uncoupling, in other words a small reduction in intercellular coupling will have a large effect on conduction velocity (Diabetic) [21]. Taken to the extreme, a large uncoupled scenario (where any decrease in intercellular coupling elicits a large reduction in conduction velocity)could eventually result in a conduction block.

1.7 Diabetes

Within the diabetic population the risk of heart failure increases from 1 to 4% (normal population) to 12% to 22% in those over 64 years [22] [23]. Studies have shown that a higher incidence of sustained ventricular fibrillation exists for diabetic rats (80%) compared to healthy rats (20%) [15]. Further, diabetics are more likely to experience heart failure after myocardial infarctions (though infarct size remains comparable) [24]. However diabetes has been shown to

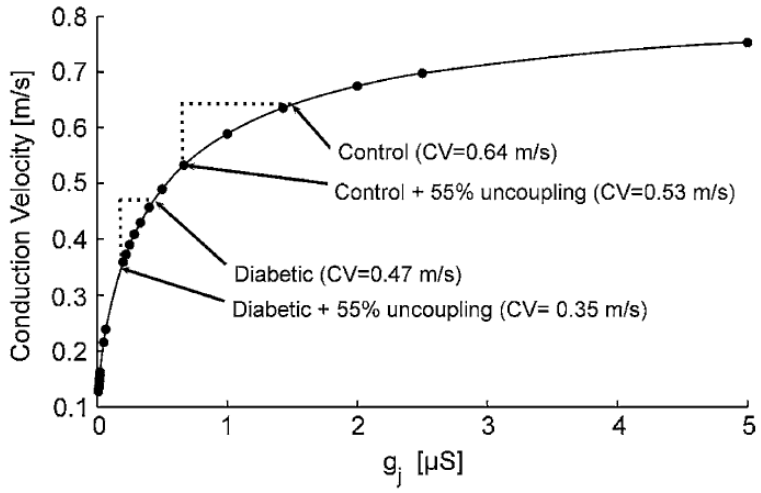

Figure 8 Relationship between conduction velocity and gap junction conductance (gj) in the one-dimensional rat ventricle conduction model. Note that the relationship ‘‘saturates’’ for increasing gj and becomes steeper for increasing degrees of uncoupling. With reasonable assumptions for baseline gj in control and diabetic hearts, as well as the degree of uncoupling produced by 0.5 mM heptanol, this relationship comes close to reproducing our experimental observations. For example, the assumptions shown above result in a 17% slowing in control hearts and a 26% slowing in diabetic hearts (compared to experimental observations of 12 and 34%, respectively). [21]

significantly decrease or completely abolish ischemia/reperfusion arrhythmias in ex-vivo rat hearts, depending on the length of time the animal was diabetic [8].

Type I diabetes down regulates and disorganizes Connexin 43, decreasing the conduction reserve [25] [26]. Western blotting of ventricular myocytes indicated that overall expression of Connexin 43 is not altered in diabetic hearts. However the organization of intercellular connections is

changed. Connexin 43 is redistributed from the ends of the cell to the sides of the cell (lateralization) (Figure 2). It is believed that this lateralized Connexin 43 is non-functional, resulting in a reduction of the conduction reserve [4].

The lateralization of Connexin 43 decreases the initial conduction reserve of the diabetic heart. As a result, a further reduction in gap junction conductance has a significant effect on conduction velocity. Previous work has shown that a significantly larger slowing of conduction velocity occurs in diabetic hearts than in normal hearts when exposed to the gap junction uncoupler heptanol or high extracellular potassium [4].

Glycogen synthase kinase-3β (GSK - 3β) activation has been shown to be two times greater in diabetic patients than in that of a control. GSK-3β activation induces cell disorganization with regards to energy and may play a key role in cardiomyopathy of diabetic tissue [27].

1.8 Ischemic Preconditioning (IPC)

The benefits of brief periods of ischemia followed by reperfusion before a large ischemic event was first reported in 1986 by Murray et al, who studied the effect of IPC in the canine myocardium. Early research shows that IPC in rat hearts protects the heart from ventricular arrhythmias [7]. In larger species IPC was shown to reduce infarct size but did not reduce ventricular fibrillation (VF) and accelerated time to VF. It is believed that the accelerated onset of VF is a result of shortened monophasic action potential duration and a decrease in the ventricular fibrillation threshold [9].

Ischemia results in the remodeling of Connexin 43 in the myocardium [10]. IPC causes a decrease in the maximum rate of uncoupling. Further rate of translocation of Connexin 43 was significantly reduced in preconditioned hearts. IPC's effect on the rate of uncoupling is related to diminished dephosphorylation and intracellular redistribution of Connexin 43 during ischemia. Both of these effects are affected by K ATP channel activation while internalization of Connexin 43 is effected by PKC. [28]

IPC has distinct effects on the interactions of Connexin 43 by affecting 3 protein kinases (Src, p38mitogen-activated protein kinase, and protein kinase C ε) during ischemia (Figure **9**). Translocation of protein kinase C ε to gap junction Connexin 43 and their complex formation is a primary mechanism of IPC-induced chemical uncoupling of cardiomyocytes during ischemia. This results in a decrease in gap junction communication as shown in Figure **9**. Further there is a suppression of Connexin 43- p38mitogen-activated protein kinase complex formation by IPC which may be a counterbalancing mechanism during the early phase of ischemia against protein kinase C ε-mediated gap junction suppression [3].

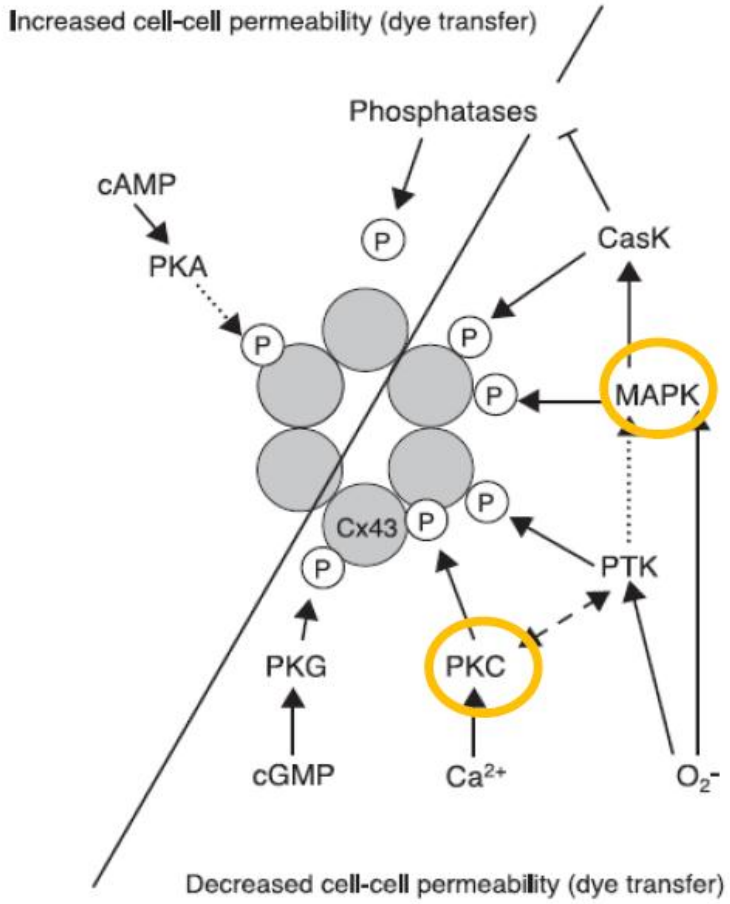

Figure 9 Schematic diagram of protein phosphatases and protein kinases (PK) on opening or closure of connexons. PTK: protein tyrosine kinase; MAPK: mitogen activated protein kinases; CasK: casein kinase; P indicates phosphorylation. **[29]**

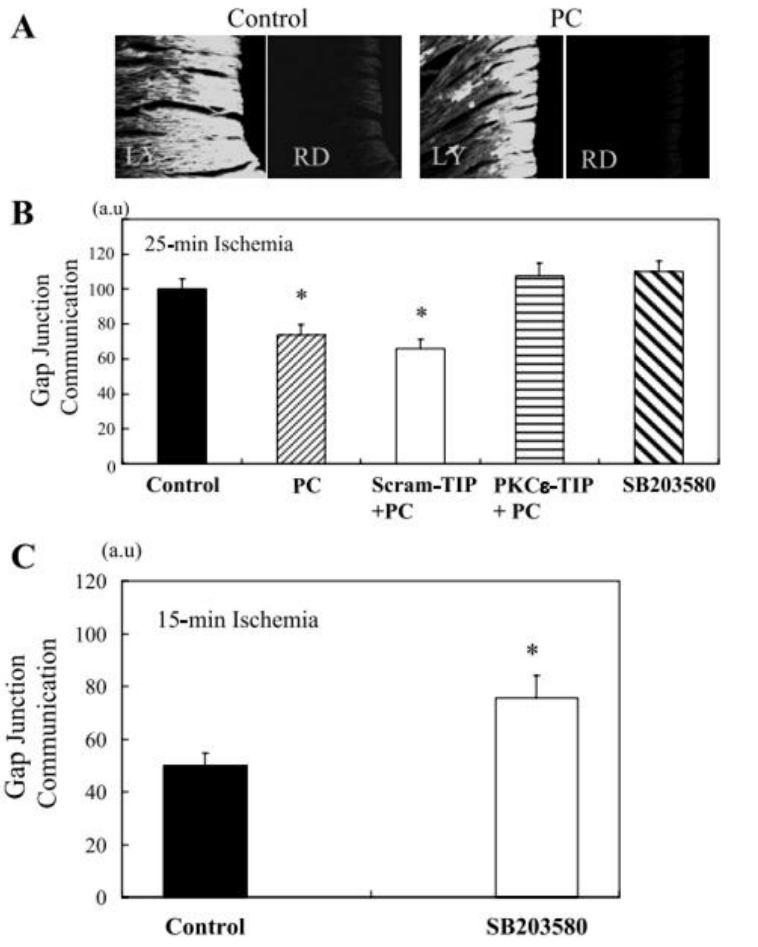

Figure 10 Effects of PC and SB-203580 on gap junction permeability in ischemic myocardium. Size of area where Lucifer yellow (LY) was transported via gap junctions during ischemia ex vivo was used as an index of gap junction permeability. Areas stained with rhodamine-conjugated dextran (RD) indicate those with disruption of sarcolemma, which was made for LY loading. RD-stained areas were subtracted from LY-stained area for determination of gap junction permeability. A: representative images of the control and preconditioned hearts. B: group mean data in protocol 1 (25 min ischemia protocol). Scram-TIP, scrambled TIP. *P< 0.05 vs. control. C: Group mean data in protocol 2 (15 min ischemia protocol). N=3~6 in each group. **[3]**

1.9 Similarities Between IPC and Diabetes:

1.9.1 Connexin 43

Diabetes is shown to induce gap junction lateralization [4], causing a decrease in the conduction reserve of the tissue. IPC has been shown to display a similar lateralization of gap junctions [3]. Both of these studies evaluated cell to cell gap junctions which connect the intracellular fluid of neighboring cells.

A recent study shows cardio protection by IPC is abolished in Connexin 43 (Connexin 43)-deficient mice due to loss of Connexin 43 located in mitochondria. Mitochondria Connexin 43 connect the mitochondrial matrix directly to the intracellular space of the cell. In a cholesterol-fed group total Connexin 43 content remained unchanged while mitochondrial total and dephosphorylated Connexin 43 content decreased. IPC was shown to reduce infarct size in normal rats but not in cholesterol-fed rats. Cholesterol fed groups develop hyperlipidemia, which can induce diabetes [30]. There is a loss of cardio protection by IPC in hyperlipidemia (considered pre-diabetic) which is associated with a redistribution of both sarcolemmal and mitochondrial Connexin 43. Figure 11 shows the level of mitochondrial Connexin 43: cholesterol-fed rats had a reduced mitochondrial Connexin 43 and IPC appears to have no noticeable further reduction (Figure 11) [31].

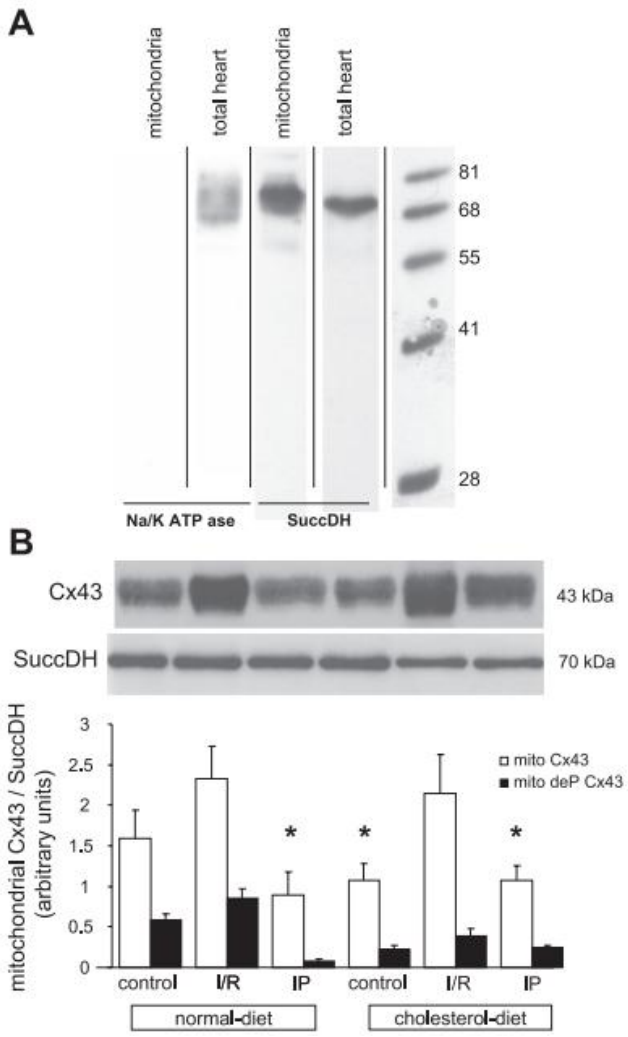

Figure 11 Mitochondrial Connexin 43 in control, I/R, and IP rat hearts. A: Western blot analysis of the isolated mitochondria and total heart samples for anti-Na-KATPase (specific for plasma membrane) and anti-succinate-dehydrogenase (specific for mitochondria). B: Connexin 43 and succinate-dehydogenase protein level in mitochondria isolated from all groups. Bar graphs represent the mitochondrial Connexin 43/succinate-dehydrogenase (SuccDH) level in all groups. Data are means SE. *P < 0.05 vs. normal-diet control, two-way ANOVA; n = 6 in each group. **[31]**

1.9.2 Arrhythmia Score

Both IPC and diabetes have been shown to have a lower number of arrhythmic animals [7] [8], IPC also has a shorter ventricular tachycardia interval. In addition to these similarities, the additive effect of IPC to diabetes resulted in no arrhythmic animals. Similarly infarct size was reduced in both pathologies, with the dual pathology subjects trending towards an additive effect, though no statistical significance is shown. [32]

1.9.3 iPLA2

In both diabetes and IPC, the activity of calcium-independent phospholipase A2 (iPLA2) is known to be increased [5] [6].

iPLA2 is a member of a family of phospholipases. These enzymes catalyze the hydrolysis of phospholipids. The family contains four subgroups including A1, A2, C and D, of which A2 is most important to the myocardium. Phospholipase A2 is responsible for the hydrolysis of the fatty acyl group at the sn-2 position of glycerophospholipids. This hydrolysis releases free fatty acid and a lysophospholipid. Both of these products are active signaling molecules within the cell. Activating PLA2 alters the structural and functional properties of the myocardium. [33]

iPLA2 is a calcium independent PLA2 enzyme [33]. Activation of iPLA2 is involved in a number of pathologies including diabetes and ischemia. iPLA2 is ATP sensitive: ATP stabilizes the iPLA2/phosphofructokinase complex, increasing the activity by a factor of 2 to 5 [34].

Up-regulation of iPLA2 resulting in an increase of fatty acid and lysophospholipids. The fatty acids then react with 2-arachidonoyl lysophospholipid to create arachidonic acid (AA) (Figure

12). Accumulation of AAs has been shown to alter the electrophysiological properties of the myocardium. Increased AA is linked to reduction in conduction velocity and prolongation of the action potential [35].

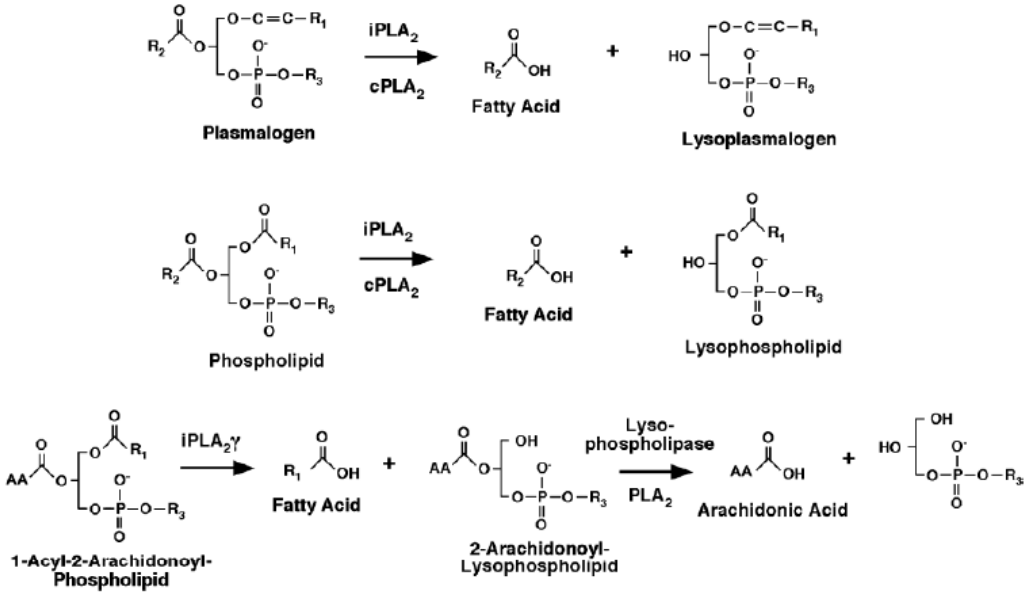

Figure 12 Intracellular phospholipids (iPLA2 and cPLA2) mediate the release of fatty acids and the production of lysolipids from membrane phospholipids. [36]

iPLA2 has been connected to the activation of store operated cation (SOC) channels as well as Ca2+ release activated channels (CRAC) implying that iPLA2 plays a key role in Ca2+ storage. [37]

1.10 Differences Between IPC and Diabetes:

1.10.1 Infarct Size

Hyperglycaemia has been shown to be a determinant on the extent of infarction in dogs. Infarct size is linearly related to blood glucose concentrations during acute hyperglycemia as well as

diabetic hearts with or without IPC. IPC is shown to significantly decrease infarct size in normal hearts while diabetes minimizes the effect of IPC on infarct size resulting is infarct size closer to control animals [38].

1.10.2 Mitochondria Permeability Transition Pore:

Physical damage, buildup of toxins, aging and any number of pathologies can lead to cell death. However there are few mechanisms of cell death. The Mitochondria permeability transition pore (MPTP) is one of these mechanisms. The MPTP is a channel which connects the mitochondrial matrix to the cytosol of the cell (which surrounds the mitochondria). The MPTP remains closed at times of physiological health with in the cell. However the MPTP can be opened during periods of ischemia and has an integral role in apoptosis (cell death).

The protein glycogen synthase kinase-3β (GSK-3β) has been directly linked to MPTP opening. Environmental stresses converge onto the GSK-3β to trigger or inhibit cell death through the MPTP [39]. Inhibition of GSK-3β prevents the MPTP from opening in reaction to environmental stresses. Figure 13 illustrates how these pathways converge onto the GSK-3β to activate or inhibit MPTP from opening.

Figure 14 shows the effects of IPC and Diabetes on cell death. IPC's inactivation of GSK-3β is hindered by diabetes higher activation of GSK - 3β. GSK-3β activation leads to opening of the MPTP [27].

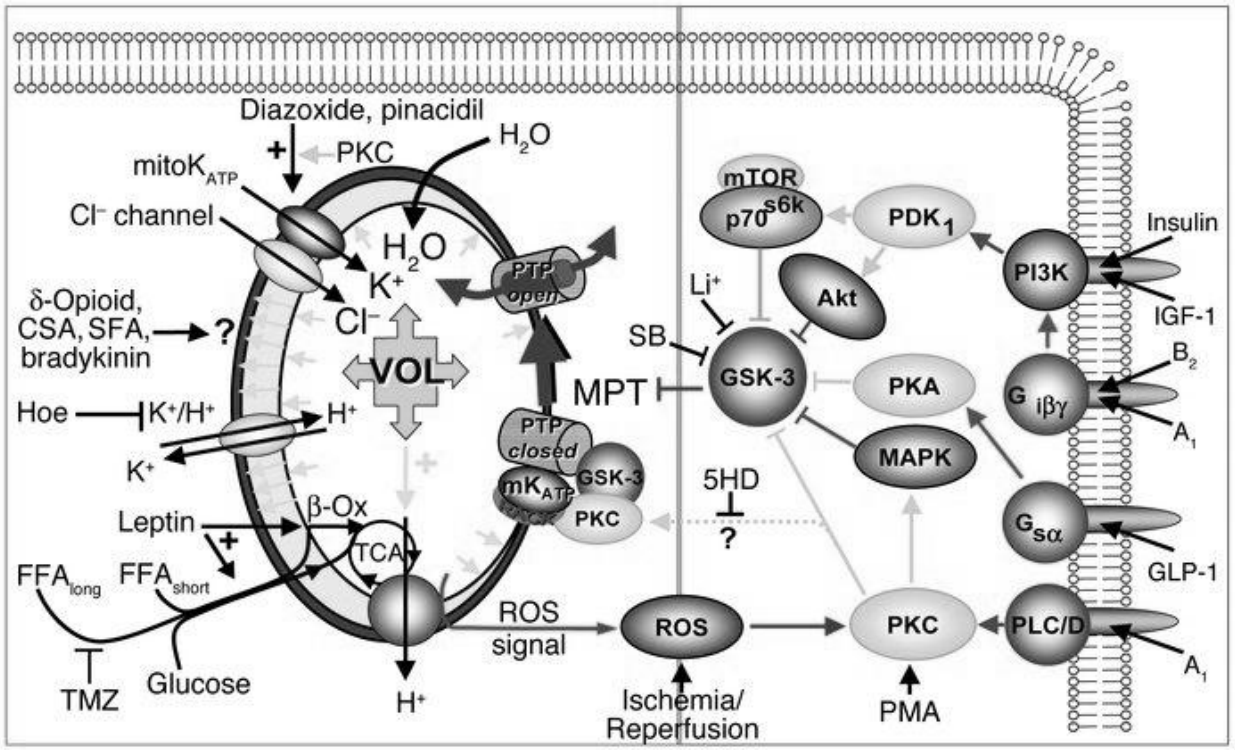

Figure 13 The integrated pathways of protection. Schematic showing the principal mechanisms: pathways dependent on change in mitochondrial volume ("swellers" such as Dz, pinacidil, leptin, DADLE, Hoe, and cyclosporin A; left, outlined in red) and pathways independent of change in mitochondrial volume ("nonswellers" such as PMA, insulin, IGF-1, CCPA, GLP-1, Li+ , SB 216763, and SB 415286; right, outlined in blue). The convergence of these pathways via inhibition of GSK-3β on the end effector, the permeability transition pore (PTP) complex, to limit MPT induction, is the general mechanism of protection. VOL, volume; β-Ox, β-oxidation; TCA, tricarboxylic acid cycle; PLC/D phospholipase C and phospholipase D. **[39]**

Inactivation of GSK-3β would mimic IPC cardio protection and override the diabetic neutralization of IPC [40]. Further it showed that using a MPTP activator would abolish any cardio protection afforded by IPC or GSK-3β inactivation (Figure 14). LiCl, IND and SB are all GSK-3β inactivators, which suppress the MPTP from opening. ATRA, however, opens the

MPTP and thus overrides any projection afforded by GSK-3β inactivation either chemically or via IPC. This work clearly indicates that MPTP inactivation is key to IPC's cardioprotective effect on cell death as well as how diabetes abolishes the effect.

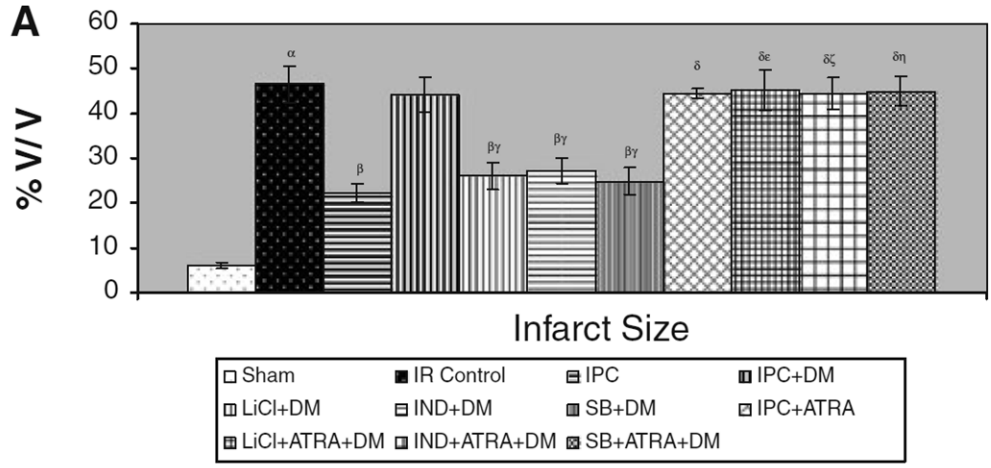

Figure 14 A Effect of ischemic preconditioning (IPC), and atractyloside in ischemic preconditioning (IPC + Atra), on ischemia-reperfusion induced myocardial infarct size in isolated normal rat heart. The effect of ischemic preconditioning (IPC), GSK-3b inhibitors (Licl, IND, and SB), induced preconditioning and atractyloside in GSK-3b inhibitors (Licl + Atra, IND + Atra, and SB + Atra), induced preconditioning on ischemia-reperfusion induced myocardial infarct size in isolated perfused diabetic rat heart. The values are expressed as mean ± SEM. a $P<0.05$ vs. sham control; b $P<0.05$ vs. I/R control, c $P<0.05$ vs. IPC in DM, d $P<0.05$ vs. IPC in normal rat heart, e $P<0.05$ vs. LiCl preconditioning in DM, f $P<0.05$ vs. Indirubin-3 monooxime preconditioning in DM, g $P<0.05$ vs. SB216763 preconditioning in DM. Adapted from [40]

Chapter 2 Methodology

To test each hypothesis three stages of lab work were completed. In each stage four groups of rats were tested: control, IPC, streptozotocin induced diabetes (STZ), and IPC + STZ.

Experiment 1 used electrocardiogram (ECG) recordings from Langendorff perfused rat hearts during ischemia-reperfusion to quantify the incidence of arrhythmias. The arrhythmias were categorized based on the criteria given in the Lambeth Conventions (discussed below).

The second and third stage utilized optical mapping measurements to assess conduction reserve of each group. The ventricular activation time in response to an electrical stimulus near the base of the ventricle was measured using optical recordings. Experiment 2 evaluated the change in activation time in response to ischemia while the third experiment evaluated changes in conduction velocity due to intercellular uncoupling.

2.1 Equipment

Figure 15 shows the block diagram of the imaging system to be used. A 250-W Quartz Tungsten halogen light source is used. The light is reflected off a cold mirror and filtered, allowing only 500± 25 nm light to pass. The light is then directed onto the preparation (epicardial surface of isolated hearts) using a dichroic mirror. When a dye (Di-4-ANEPPS) is excited, it fluoresces a light proportionally to the cell's membrane potential. The red light emitted from the preparation is filtered through the dichroic mirror and a long wave pass filter (>590nm Schott glass) before it reaches the CCD camera.

The light source and camera shutter are automated for optical recordings by the Lab View data acquisition software, which isolates the light exposure to the heart to the recording time [41]. The camera produces a 15×15 mm field of view (250×250μm/pixel) and is connected to a National Instruments PCI-1422 image acquisition board. The data acquisition board is responsible for all collected data.

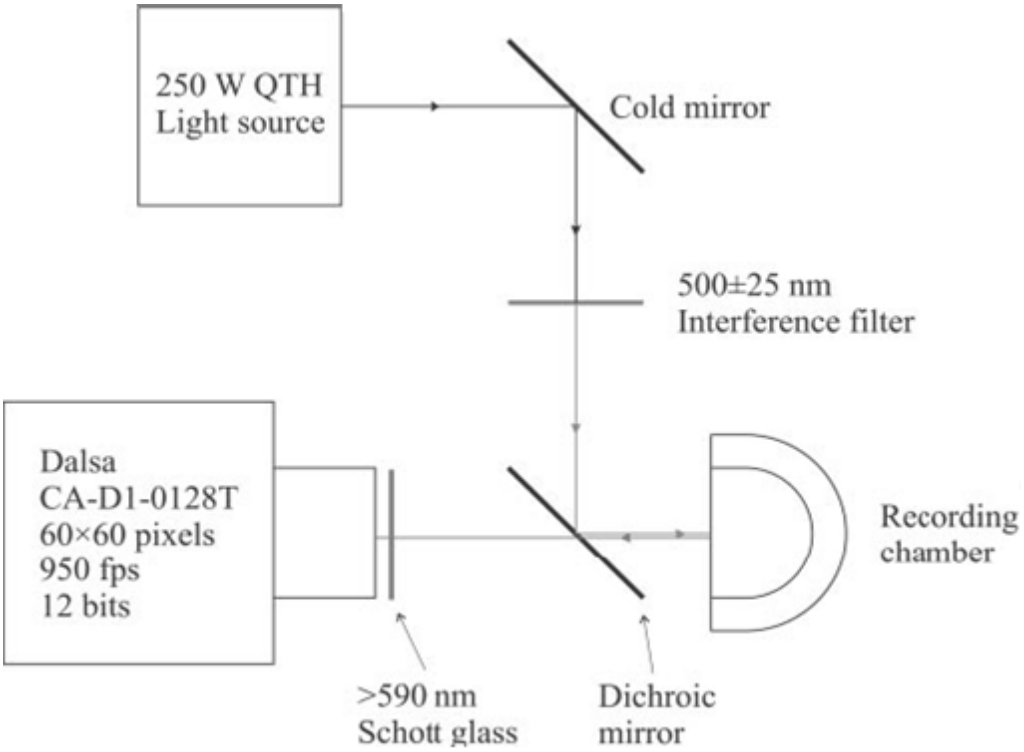

Figure 15 Block diagram of optical mapping hardware. Light travels from the light source to the tissue in the recording chamber. The light emitted by the electrically excited dye travels through the filter and is recorded via the Dalsa camera. **[41]**

2.2 Data Collection

Pressure, temperature, stimulation pulse, and the three ECG signals were recorded throughout the experiment beginning 20 minutes before the experimental protocol was initiated. The three ECG signals were generated by subtracting the electrical potential of one of the surface

electrodes from that of another in accordance with the classical ECG (all three lead channels were collected). Optical mapping data is collected in 5 second time intervals. The data recording at each time was synchronized to ECG and stimulus pulses by software written in Lab View [41].

2.3 Optical Mapping Recordings

To obtain optical mapping data, all animals were sacrificed and their hearts maintained ex-vivo via Langendorff Perfusion. For optical mapping protocols the optical mapping dye (Di-4-ANEPPS) was added after a 20 minute normalization period. After normalization the dye was added for 5 minutes, followed by a 10 minute wash out.

Di-4-ANEPPS was diluted from a 10 mM stock solution in DMSO to a 1μM concentration in the K-H buffer solution. An initial "test" optical recording was taken. Di-4-ANEPPS was used because it is able to follow the changes across a cell membrane on a millisecond timescale. The dye absorbs 500±25 nm and emits a longer wavelength (>590 nm) fluorescence light, the intensity of which is proportional to the voltage across the cell membrane (Efimov et al, 2004). Early tests during experimentation showed that Di-4-ANEPPS changed the ECG in control animals. For this reason, any tissue treated with Di-4-ANEPPS was not used for evaluation of Ischemia/Reperfusion arrhythmias. Recently Di-4-ANEPPS has been shown to significantly slow the conduction velocity of myocardial tissue [42],

For the optical recordings to be of use for our purposes, the SA node of the heart had to be overridden. For this reason the heart was paced using a fixed current signal (amperes used were subject dependent) with a pulse cycle of 200 ms. The pacing current was initiated at 1μA and

increased until the pacing induced tissue activation, overriding sinus rhythm. Once the minimum pacing current needed (threshold) was determined, the pacing current was set to twice threshold for the remainder of the experiment. If the current became insufficient for initiating tissue activation then the current was again increased until activation occured. The pulsing rate was only increased if the hearts natural rhythm was occurring before the pacing signal. Pacing only occurred immediately before and during optical recordings. The heart was otherwise allowed to beat in conjunction with the sinus atrial node firing (sinus rhythm). The heart was never paced when entering or exiting IPC (preliminary tests showed this to induce reperfusion arrhythmias).

The tissue is paced to ensure that tissue activation is conducted on the 2 D surface of the front of the heart, which is recorded by the optical mapping equipment. Orientation varies widely through the depth of myocardium [43]. The varied orientation of myocardium in ventricle tissue complicates measurement of conduction velocity in the tissue. There is not a simple method to measure longitudinal or lateral conduction velocity.

2.4 Excision of Heart

Animals were injected with approximately 0.7 mL of 300 U heparin (an anticoagulant) 10 minutes before extraction of the heart begins. Treatment with heparin prevents induced ischemic regions in the heart after extraction due to blood clotting.

10 minutes after heparin injection, the rat was placed in a small chamber where it was delivered pure oxygen and isoflurane gas at a flow rate of 1000 ml/min. The gas mixture put the animal to sleep at which time it was weighed and moved to a mask delivery system with a flow rate of 700 (mL/min) of the 5% isoflurane, 95% oxygen. The rat's responses were checked to ensure the

animal was unconscious. The fur on the chest of the animal was removed, then the rib cage was cut, starting below the xiphoid process and moving superiorly until only the top 20% of the rib cage remained attached. The ribs were lifted, exposing the heart. The aorta was then severed and the heart was quickly transferred to an ice cold Krebs-Henseleit buffer (K-H buffer) solution. The heart was then promptly moved to the Langendorff perfusion apparatus. Methods were approved by the University of Calgary Health Science Animal Care Committee.

2.5 Langendorff Perfusion

The aorta was cannulated and mounted vertically and perfused with K-H buffer heated to a temperature of 37ºC at a constant flow rate of 7 ml/min (delivered by peristaltic pump). The perfusion pressure in the cannula was monitored with a pressure transducer connected to the cannula and recorded throughout the experiment. Flow was adjusted if pressure continuously increased or was too low. A normal pressure was generally between 25 and 100 mmHg.

The K-H buffer consisted of the concentrations listed in Table 1. The solution was warmed in a water bath set to 37 ºC while gassing with 95% O2 and 5% CO2 to maintain a constant pH (7.4). The K-H buffer was passed through a glass heated coil to maintain 37º C before reaching the heart.

The heart is then immersed in K-H buffer solution in the chamber. The temperature in the chamber is monitored using a thermocouple thermometer and maintained at 37º C. The chamber has two adjustable side supports and one inflatable balloon behind the heart; these are used to help position the heart as well as reduce motion artifacts caused by the tissue contracting.

Table 1 List of compounds of K-H buffer and their corresponding concentrations. A stock solution 10 times desired concentration consiting of all compounds except NaHCO, Dextrose and CaCl2 is kept on hand. On the day of testing the solution is diluted, missing compounds are added and the K-H buffer is placed in the warming bath and gassed in preperation for the Langendorff perfusion.

Compound	**Concentration (mM)**
NACl	118.5
$NaHCO_3$	25.0
KCl	4.7
$MgSO_4$	1.2
KH_2PO_4	1.2
CaCl2	2.0
Dextrose	11.0

2.6 Surface Electrodes

Three surface electrodes were sutured at the left ventricular base, right ventricular base, and left ventricular apex of the heart to monitor the ECG. One pacing electrode was sutured to the heart near the base of the left ventricle to facilitate the electrical stimulation of the tissue (only for Experiments 2 and 3).

The surface electrodes were custom made. Silver wire was made into a loop and soldered onto an insulated copper wire. The silver end of the electrode was oxidized in a saturated potassium

chloride solution thus generating a silver chloride coating. This coating reduces the noise generated due to movement. ECG data was recorded at a rate of 950 Hz.

2.7 Data Processing

Optical mapping data was initially analyzed during the experiment for quality purposes only. All data processing occurs after the completion of the experiment.

ECG data was evaluated starting 5 minutes before IPC or the 25 minute normalization. The first 30 seconds of each ECG recording was evaluated in 0.1 time intervals. For each interval the number of normal ECG signals was recorded, as well as the number of bigeminy beats, ventricular premature beats, systolic beats, tachycardia events, and fibrillation events, as defined by the Lambeth Convention (see below).

2.8 Lambeth Convention

The Lambeth conventions are guidelines intended to standardize how arrhythmias are quantified (Figure 16). Arrhythmias may be caused by anything, including: ischemia, infarction or reperfusion. For an intact sample all data required to quantify the arrhythmia is obtained from the ECG. [44]

Ventricular premature beats (VPB)

- Defined discrete and identifiable early QRS complexes.
- The beat is premature in relation to the P wave.

Bigeminy (abnormal heart beat in every other beat)

- May be electro physiologically different than VPB.
- Is to be specified as a variant of the irregular VPB.

Ventricular tachycardia (VT)

- Defined as 4 or more consecutive VPBs.
- Should only 2 or 3 consecutive VPBs occur than it should be referred to as a salvo.
- Should not be defined by rate or prevailing sinus rate. If rate were to be used then definitions would be species dependant.

Ventricular fibrillation (VF)

- Defined when individual QRS complexes cannot be identified, or when morphological instability exists and rate can no longer be measured.

Both ventricular fibrillation and tachycardia can be subdivided depending on the morphology and regularity of rate. However, subcategories should be clearly defined by the investigator and should not replace evaluations of the main categories (VPB, bigeminy, ventricular fibrillation or ventricular tachycardia). Further subcategories will often result in the need for larger sample sizes for significant results to be found. [44]

An arrhythmic score is any ranking scale that is applied to raw data. It does not include derivatives of raw data. While many scoring systems exist, the assumptions each system makes are important. [44]

From the optical mapping data, time of activation for each pixel (with respect to the stimulus pulse) was calculated. For each beat an activation map was computed with each pixel's activation time. The average time of activation for each individual pixel over all beats in a recording (5 seconds, approximately 10-25 beats) was calculated, resulting in signal-averaged times of activation and an averaged activation map (Figure 17). The overall measure of

activation time can be determined from a histogram with the activation times of each pixel in the averaged activation map. The width of the histogram is taken as the overall activation time for the heart.

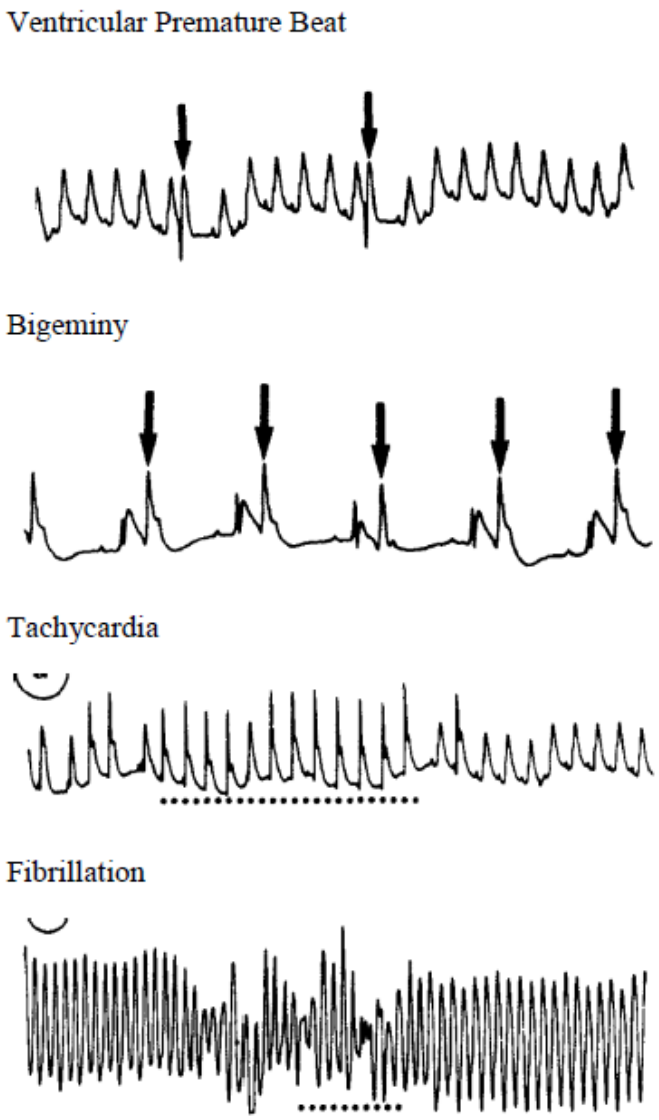

Figure 16 An illustration of the four arrhythmias categorized in the Lambeth Conventions. Adapted from [44].

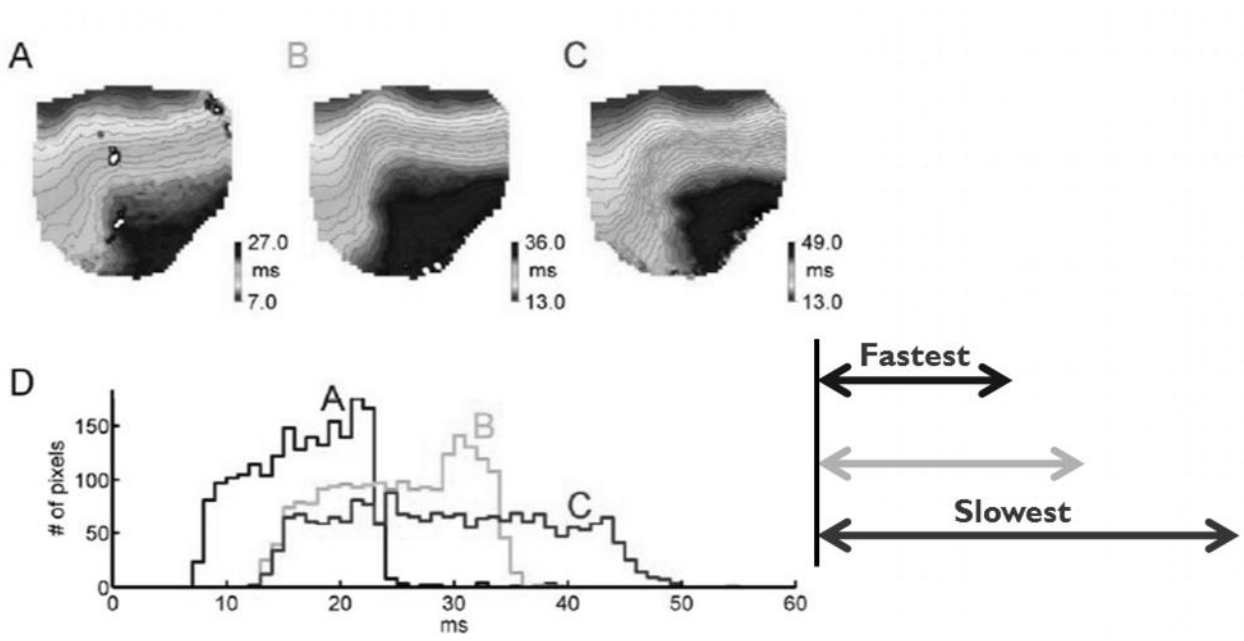

Figure 17 Optical activation maps and corresponding histograms. A, B and C are optical maps of the activation times of individual pixels of the heart image. Each optical map is an average of a 20 or more consecutive action potentials. A, B, and C are the same heart at different times of the experiment. To eliminate background, a mask is placed on the optical map removing areas of the image that is not the desired heart tissue. Using the activation times of each pixel a histogram is generated for each map. The width of each histogram is taken as the total activation time for the tissue. As variance occurs in physical size between subject the total activation times are normalized to a initial reference recording (B and C are normalized to A). Adapted from **[5]**.

Overall activation times are normalized to the baseline recording taken before an intervention was applied. This results in a measure of the change in conduction velocity for a recording with respect to its baseline. [41]

2.9 Arrhythmia Scoring

The scoring system used in this work is displayed in Table 2. The scoring system differentiates between duration and type of arrhythmia. [45]

Table 2 Scoring system "A" used on ischemia/reperfusion arrhythmias. **[45]**

Score	Arrhythmia
0	0 to 49 VPBs over the 60 minutes
1	50 to 499 VPBs over the 60 minutes
2	Greater than 499 VPB over the 60 minutes or 1 episode of reverting VT or VF
3	More than 1 episode of VT of VF less than 60 seconds of duration
4	VT or VF between 61 and 119 seconds in duration
5	VT or VF greater than 119 seconds in duration
6	Fatal (continuous) VF starting 15 minutes or later after reperfusion
7	Fatal (continuous) VF starting between 4 minutes and 15 minutes after reperfusion
8	Fatal (continuous) VF starting between 1 minute and 4 minutes after reperfusion
9	Fatal (continuous) VF starting before 1 minutes after reperfusion

2.10 Healthy Controls

Healthy controls were male Sprague-Dawley rats (225–350 g).

2.11 Ischemic Preconditioning (IPC)

Healthy controls were subjected to the IPC protocol. IPC began twenty five minutes prior to the heart being subjected to a physiological stressor (ischemia for Experiments 1 and 2, and high extracellular K^+ for Experiment 3). IPC consisted of 2 cycles of 3 minutes global ischemia (the

perfusate pump was turned off). Followed by five minute reperfusion after the first IPC and a 10 minute reperfusion followed the second.

2.12 Diabetes Inducement

Healthy animals were made STZ diabetic by giving injections of STZ (65 mg/kg) 7 to 14 days before testing. STZ injections consisted of 65 mg/kg STZ dissolved in equal volumes citrate buffer (1 mL/kg) and saline. The STZ solution was injected subcutaneously within the first 7 days of the arrival of the healthy controls. During the extraction of the heart, the diabetic state of each animal was confirmed using a glucometer. The glucometer measured blood glucose levels in mmol/dL. Blood glucose greater than 20 mmol/dL was considered diabetic. If the blood glucose of an STZ-treated animal was below 20 mmol/dL the data was excluded from analysis.

2.13 Experiment 1 Ischemia-Reperfusion Arrhythmias

Experiment 1 compares the ischemic/reperfusion anti-arrhythmic effects of the two pathologies.

Shahir Mishriki was responsible for the majority of the data collection, in addition to the time to flat line and ischemia/reperfusion arrhythmia time analysis for the data he collected as part of a summer student project. All additional analysis was done by Alyssa Randall. See Appendix A for further details.

2.13.1 Protocol

The heart was extracted and perfused using Langendorff perfusion. There is a 35 minute stabilization period to match the durations of Experiment 2 and 3. The heart either underwent IPC or was left to normalize for an additional 21 minutes. Global ischemia was induced by turning off the peristaltic pump. ECG recording occurred continuously throughout the

experiment. After 30 minutes of ischemia, the peristaltic pump was turned back on for 60 minutes or reperfusion.

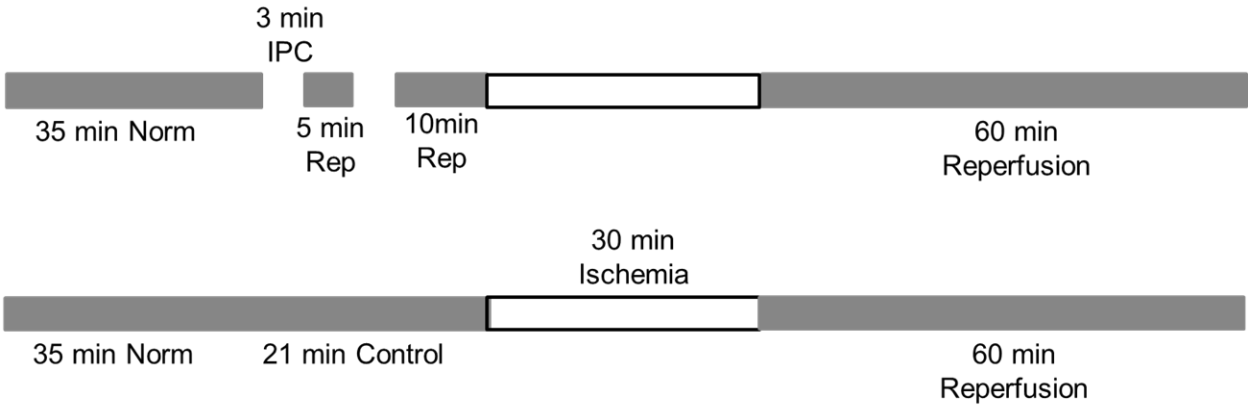

Figure 18 Illustration of Experiment 1 Protocol for either IPC or time matched control. Subject may or may not be STZ induced diabetic at the time of the experiment. If STZ diabetic then the subject would be referred to as STZ + Control or STZ + IPC depending on protocol.

2.13.2 Analysis

Each subject's ECG data was analyzed for the following:

a. Length of time until heart flat lines during ischemia.
b. Heart Rate during ischemia, measured by R-R interval length.
c. Conduction velocity of tissue during ischemia, measured by QRS interval time.
d. Conduction velocity slowing of tissue during ischemia, measured by change in QRS interval time.
e. Reperfusion arrhythmias throughout reperfusion. This is used to quantify the fraction of time each heart spends in any arrhythmic state with respect to time and determine an arrhythmic score for each animal.
f. Correlation between time to flat line and arrhythmia score.

2.14 Experiment 2 Activation Times During Ischemia (Paced)

This experiment was designed to evaluate the tissue's response to ischemia using optical mapping. This had to be done separately from the ischemia/reperfusion protocol of Experiment 1, as initial experiments showed di-4-ANEPPS changes conduction properties of the heart and the stress of pacing the heart results in a flat line earlier than that of sinus rhythm.

Experiment 2 used control and STZ raw data collected by Parisa Rahnema for her thesis titled *Cardiac Impulse Propagation in Diabetic Heart: Response to Oxidative Stress and Ischemia*. Additional control and STZ data was collected to supplement the set. All data was processed by Alyssa Randall. See Appendix A for further details.

2.14.1 Protocol

After treatment with the voltage dye, the heart underwent either IPC or the corresponding 21 minute normalization period. In the last 2 minutes of this phase an optical mapping recording was taken.

The peristaltic pump was then turned off (causing a final period of ischemia). An optical mapping recording was taken after one minute ischemia and again at each subsequent minute until the heart flat lined or fibrillation was sustained for more than 60 seconds. Pacing was maintained throughout ischemia due to the high frequency of optical recordings.

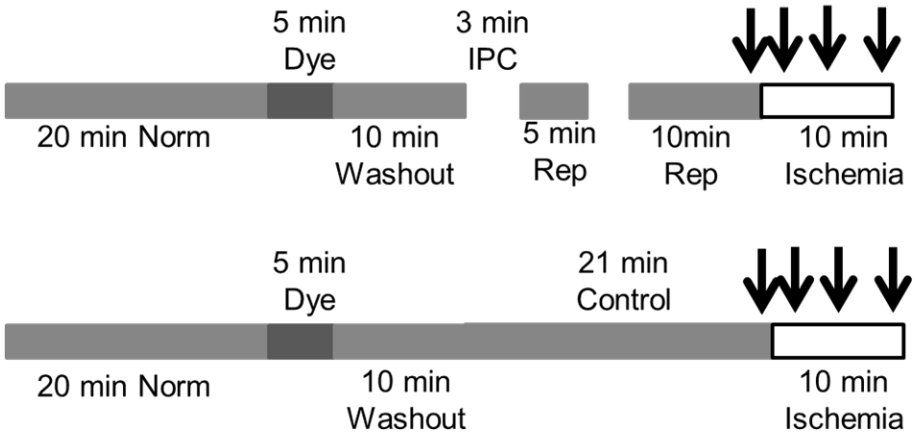

Figure 19 Illustration of Experiment 2 Protocol for either IPC of time matched control. Subject may or may not be STZ induced diabetic at the time of the experiment. If STZ diabetic then the subject would be STZ + Control or STZ + IPC depending on protocol. Black arrows indicate Optical Mapping recordings that were analyzed (0, 2, 5 and 10 minutes ischemia). Once final ischemia begins, optical mapping will only occur if the heart is not in fibrillation or flat lined.

2.14.2 Analysis

a. Effect of IPC protocol on tissue activation time (using optical mapping data) for STZ and control animals.
b. Effect of ischemia on tissue activation time over the first 5 minutes of ischemia.
c. Rate of slowing of activation time over first 5 minutes of ischemia.

2.15 Experiment 3 Conduction Reserve (Response to High K^+)

Experiment 3 exposes the hearts to high [K^+] (9mM). High extracellular K^+ is a physiological stressor which slows the conduction velocity of the tissue.

Experiment 3 used control and STZ raw data collected by Shimoni for *Sex-dependent impairment of cardiac action potential conduction in type 1 diabetic rats*. Data was

supplemented with additional animals to obtain statistical significance. All data was processed and analyzed by Alyssa Randall. See Appendix A for further details.

2.15.1 Protocol

Following treatment with the optical dye, the heart underwent either IPC or a 21 minute normalization period. At 0 to 2 minutes before treatment with high [K^+], an optical recording was taken.

The heart was exposed to 9mM high extracellular K^+ for 10 minutes, at the end of which a second optical recording was taken.

2.15.2 Analysis

For each subject, the changes in activation times for tissue with reduced excitably due to high extracellular K^+ were analyzed.

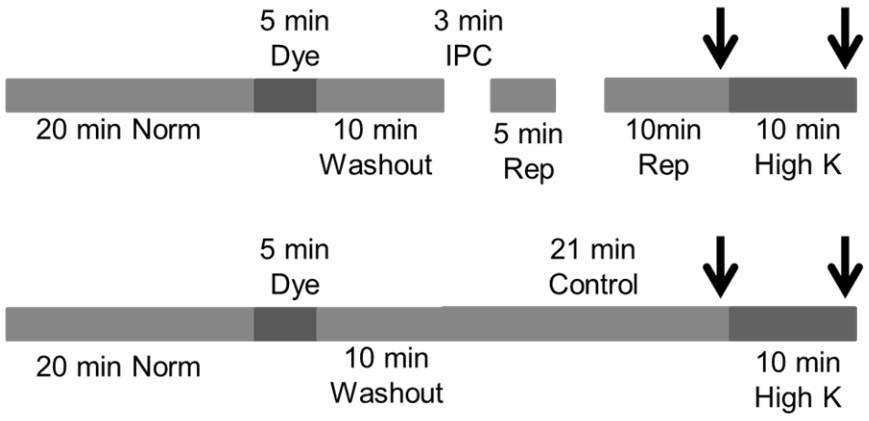

Figure 20 Illustration of Experiment 3 Protocol for either IPC of time matched control. Subject may or may not be STZ induced diabetic at the time of the experiment. If STZ diabetic then the subject would be STZ + Control or STZ + IPC depending on protocol. Black arrows indicate

Optical Mapping recordings. Once high K+ begins, optical mapping will only occur if the heart is not in fibrillation or flat lined.

2.16 Sample Size Calculation

Sample size was estimated based on previous optical mapping rat model studies comparing diabetes to controls. Data was collected and processed on an ongoing basis to avoid using more animals then necessary to achieve a 95% confidence interval or greater.

A sample power analysis for calculating the required number of animals is shown for a 2-Tailed T-Test. Using data collected by collected by Parisa Rahnema for her thesis titled *Cardiac Impulse Propagation in Diabetic Heart: Response to Oxidative Stress and Ischemia*.

Table 3 Values for Sample Power Analysis

α	0.05
Power (1-β)	0.95
Stand Deviation of Error	0.0388
Mean (μControl)	1.96
Standard Deviation (σControl)	0.0776
Mean (μSTZ)	1.70
Standard Deviation (σSTZ)	0.0745

Given the example values in Table 3, 8 animals from each group would be used (calculation completed using G*Power 3.1.5 software). If statistical confidence greater than 95% ($p<0.05$) is found before 8 animals then no more data would be collected. Alternatively if at 8 animals the confidence is approximately 92% or greater ($p<0.08$) then 2 more animals would be completed.

2.17 Statistical Analysis:

All four groups (Control, STZ, IPC and IPC + STZ) were compared using a one way ANOVA (Analysis of Variance). A Shapiro-Wilk normality and an Equal Variance test ($p>= 0.05$) was used to define significance. If the groups were found to be significantly different by the ANOVA test, then the Holm-Sidak method of multiple comparison procedures was used. When only comparisons to a specific group were desired (Control Group) the Dunn's comparison method was used. Dunn's Multiple Comparison Test allows a number of contrasts from among a set of mean scores. Unlike Fisher, Scheffé, and Tukey, which provides methods for testing comparisons between all possible combinations of normally distributed variables, Dunn's allows only a few comparisons to be performed, thus maintaining control over an inflated Type I error.

In some cases, two groups had similar results and a third group had an average between the first two groups and the fourth. In these cases the ANOVA would often fail. If this occurred, the two groups were compared individually to each other using a two tail T-Test. Differences were considered significant only when p was less than 0.05.

Chapter 3 Results

3.1 Experiment 1 Response to Ischemia:

Experiment 1 looked at the ischemia reperfusion properties of the four groups using ECG recordings exclusively. This experiment evaluated the data for time to flat line, arrhythmia scoring, and R-R interval time as described in Methods.

The time to flatline was defined as the length of time for the ECG to stop displaying QRS complexes for 1 minute. When atrial activation remained but conduction block stopped the travel of electrical activity to the ventricals the ECG was categorized as flat line. The time to flat line was only measured during the final 30 minutes of ischemia and not throughout the IPC protocol.

As shown in Figure 21 the STZ group took significantly longer to reach flat line than control. Neither the IPC nor the IPC + STZ groups showed significant slowing to flat line. However IPC + STZ had a mean flat line time that suggested an averaging of the STZ and IPC group flat line times.

The R-R interval was measured to indicate the time between ventricle contractions. For each experiment successive R-R measurements were taken and averaged (Figure 22).

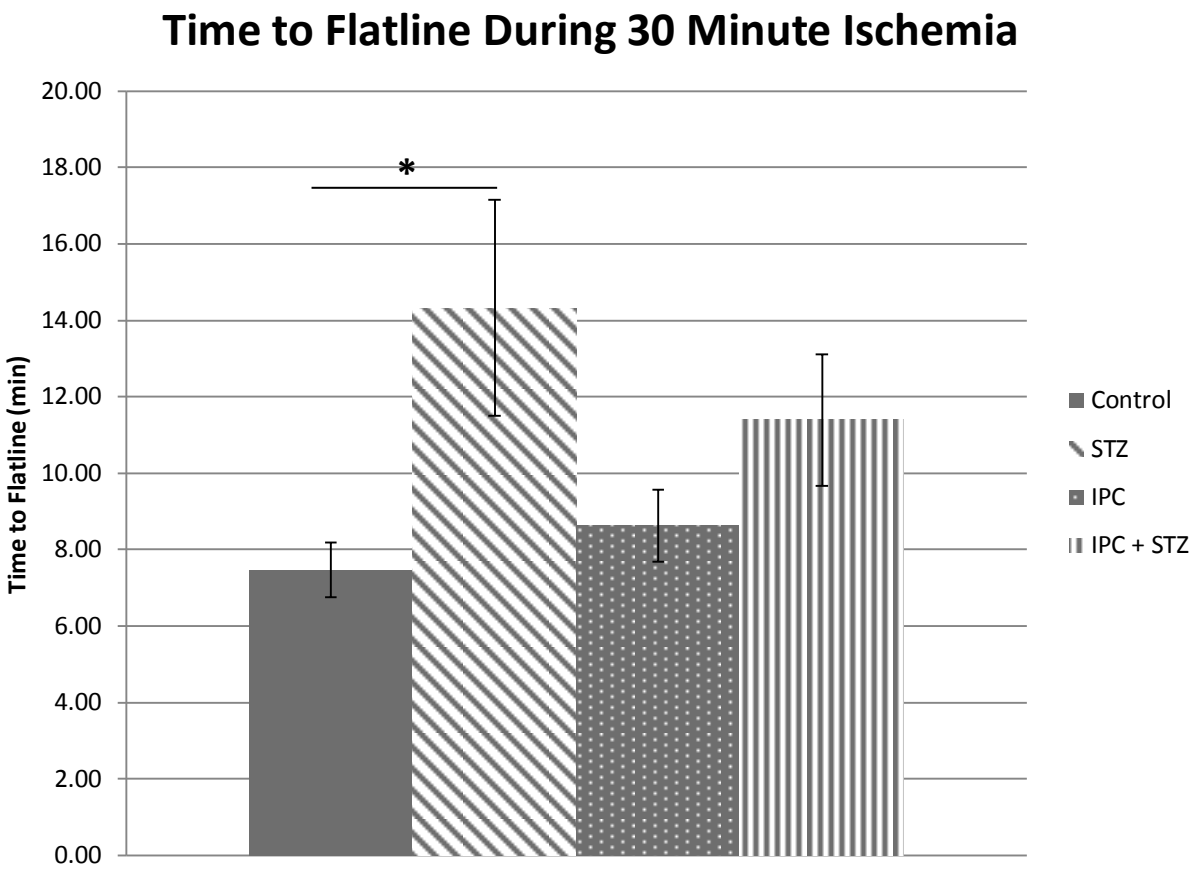

Figure 21 Time to flat line during 30 minute ischemia. The defined time of flat line is the time of the last QRS complex before contractions cease to occur until reperfusion. * indicates $p < 0.05$ using One Way ANOVA. Control n=7, STZ n=8, IPC n=6 and IPC+STZ n=8.

Throughout ischemia the R-R interval (inversely proportional to heart rate) for IPC and control are very similar while STZ has a marked increase shown to be significantly different from control at 0 and 1 minutes and from IPC at 0, 1 and 2 minutes. IPC + STZ has a lower increase in R to R interval length though it is significantly different from IPC at 1 and 3 minutes while significantly different from control at 2 minutes. IPC follows control while IPC + STZ appears to again be a combination of STZ and IPC behavior. After 3 minutes the variance within the groups make statistical significance impossible to achieve.

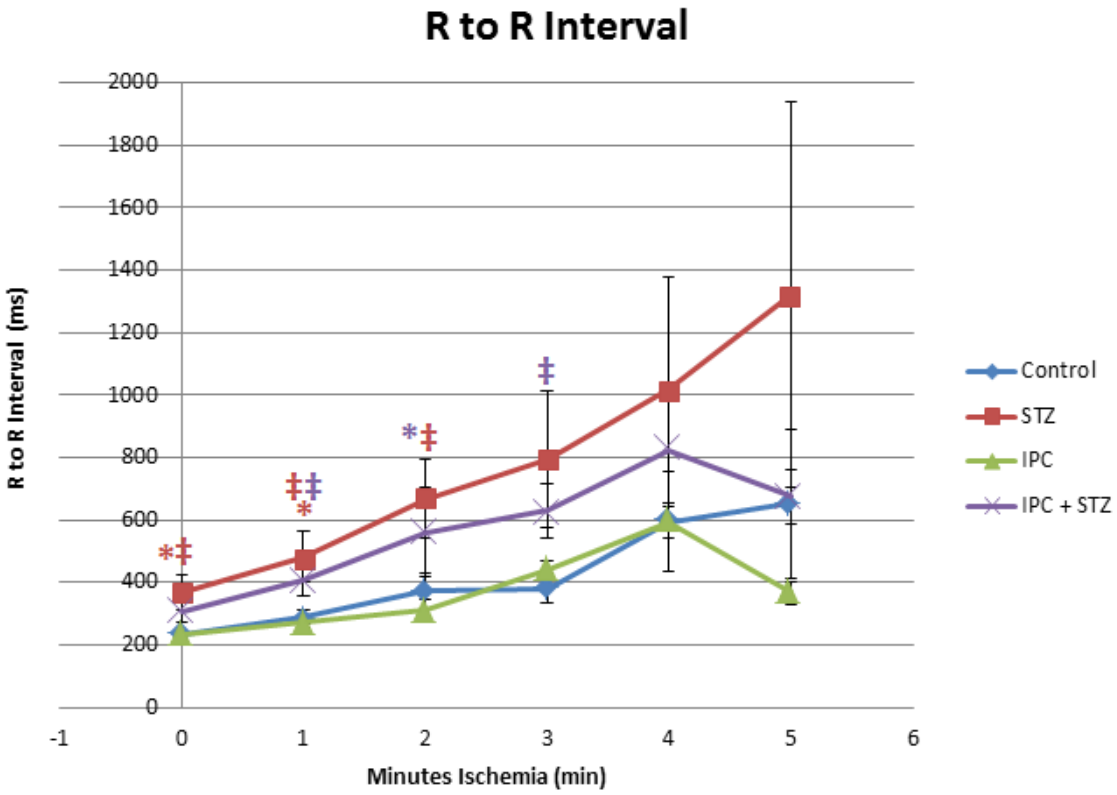

Figure 22 Time of R-R intervals during ischemia for control, STZ, IPC and IPC + STZ. * indicates a $p < 0.05$ with respect to control using two tailed t-test, while ‡ indicates a significant difference ($p < 0.05$) with respect to IPC using the same method. Control n=8, STZ n=7, IPC n=6 and IPC+STZ n=7.

The drop in R to R interval length for IPC and IPC + STZ groups at 5 minutes compared to its length at 4 minutes is due to a loss of animals for measurements and not statistically significant. Secondly the animals that did drop off had the longest R to R intervals thus elevating the averages for previous minutes as shown in Table 4.

Table 4 R-R interval times for individual animals

	Average	Average Ischemia R-R Interval Times				
	Control (msec)	1 Min (msec)	2 Min (msec)	3 Min (msec)	4 Min (msec)	5 Min (msec)
Control	228.0	253.5	285.1	322.0	382.9	1815.0
	218.2	226.5	523.6	663.6	1261.1	
	264.1	340.8	355.1	327.3	322.0	328.0
	220.4	263.3	261.8	282.2	344.6	408.5
	210.7	230.2	249.8	293.4	351.4	597.9
	254.3	267.8	281.4	292.7	306.2	333.3
	264.1	301.7	320.5	355.9	399.5	427.9
	201.6	428.1	719.6	514.6	1397.3	
STZ	265.6	327.3	455.9	629.7	786.2	973.0
	372.4	452.2	511.6	546.2	574.0	629.7
	301.7	337.1	414.5	545.5	665.1	729.8
	349.8	473.2	580.1	703.5	799.7	779.4
	264.1	528.2	1086.9			
	322.0	329.5	408.5	468.0	466.5	428.8
	705.7	935.2	1216.7	1879.6	2807.2	4386.1
IPC	218.2	240.8	273.9	297.9	336.3	437.1
	212.2	267.8	264.1	282.1	293.4	353.6
	302.4	285.1	288.9	294.9	297.3	310.0
	213.7	299.4	468.7			
	252.0	310.0	319.8	352.1	512.4	
	210.7	224.2	266.3	428.8		
IPC + STZ	212.2	267.8	300.2	997.6	1530.9	
	288.2	428.8	504.8	716.2	1111.6	889.3
	322.0	376.9	437.1	482.3	449.2	546.2
	513.1	676.4	1386.8			
	309.2	464.2	519.9	585.3	626.0	586.1
	262.6	288.9	310.7	371.7	471.0	479.2
	250.5	357.4	472.5	622.9	764.4	877.2

The time from the Q to the S wave of the tissue was measured for each group (Figure 23). Ten consecutive QRS wave forms were averaged and the measured interval length recorded for each subject. This value was normalized to the QRS length at 0 minutes ischemia to determine the slowing of the ventricular contractions due to ischemia.

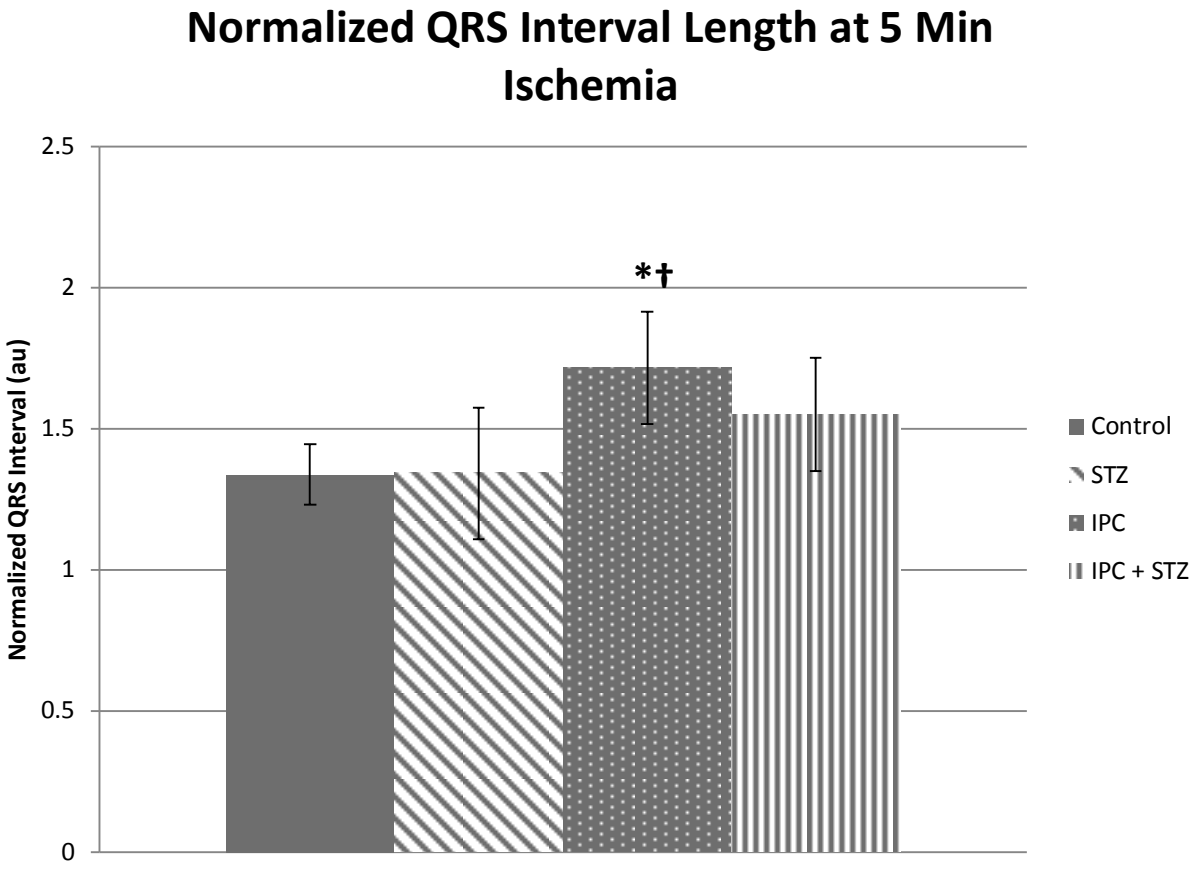

Figure 23 QRS lengthening due to ischemia for control, STZ, IPC and IPC + STZ. * denotes $p < 0.05$ significant difference from control while † denotes $p < 0.05$ significant difference from STZ using a one way ANOVA. Control n=6, STZ n=6, IPC n=6 and IPC+STZ n=4.

The IPC group has a significant increase in the lengthening of the QRS complex at 5 minutes compared to the control. STZ shows no difference from control in the lengthening of the QRS

complex while the IPC + STZ group has a slowing that is an average of the IPC and the STZ group (though not significantly different from either).

Figure 24 clearly shows that STZ animals do not have a longer QRS interval than control or IPC initially, and that the QRS interval for IPC is longer than that for STZ.

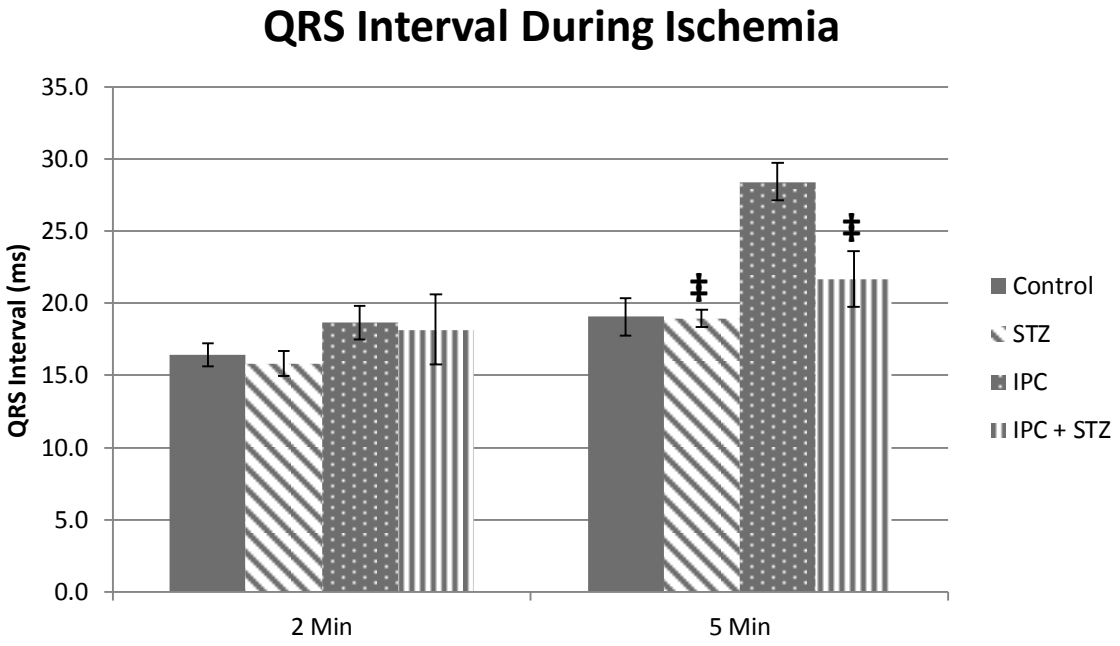

Figure 24 QRS time in ms during Ischemia for Control, STZ, IPC and IPC + STZ. ‡ denotes $p < 0.05$ significant difference from IPC using a One-Way ANOVA. Control n=6, STZ n=6, IPC n=6 and IPC+STZ n=4.

3.2 Experiment 1 Ischemic/Reperfusion Arrhythmias:

Ischemia reperfusion arrhythmia scores (Figure 25) indicate that IPC has no significant benefit while STZ does. The IPC + STZ group also indicated a significantly better arrhythmia score than control groups. As IPC had no significant effect the benefits of the IPC + STZ treatment may be attributed to STZ.

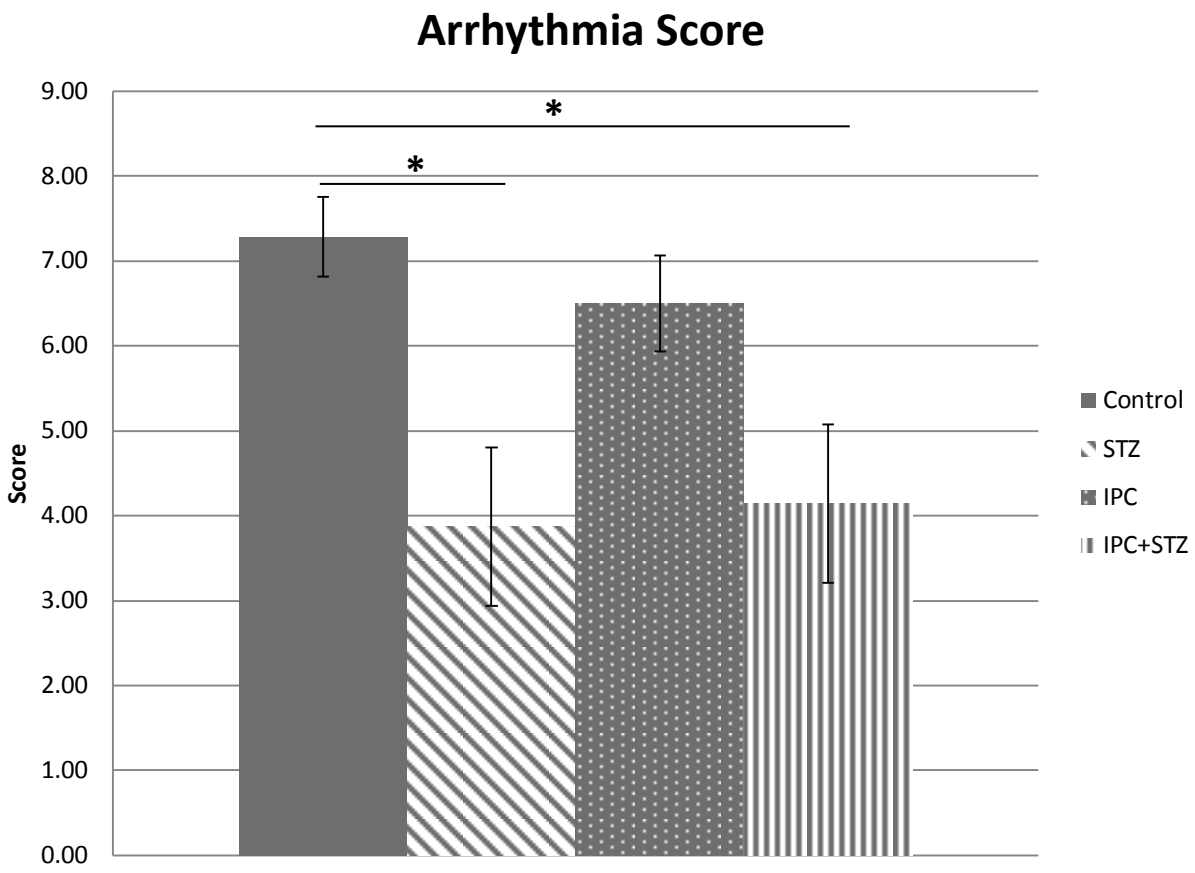

Figure 25 Arrhythmia Scores for ischemia/reperfusion arrhythmias during the first 60 minutes of reperfusion. IPC + STZ and STZ reduced the arrhythmia score by 46.8% and 43.1% respectively. * indicates $p < 0.05$ using a One-Way ANOVA. Control n=8, STZ n=7, IPC n=6 and IPC+STZ n=7.

To determine if there was a correlation between time to flat line and Arrhythmia scores Figure 26 was created.

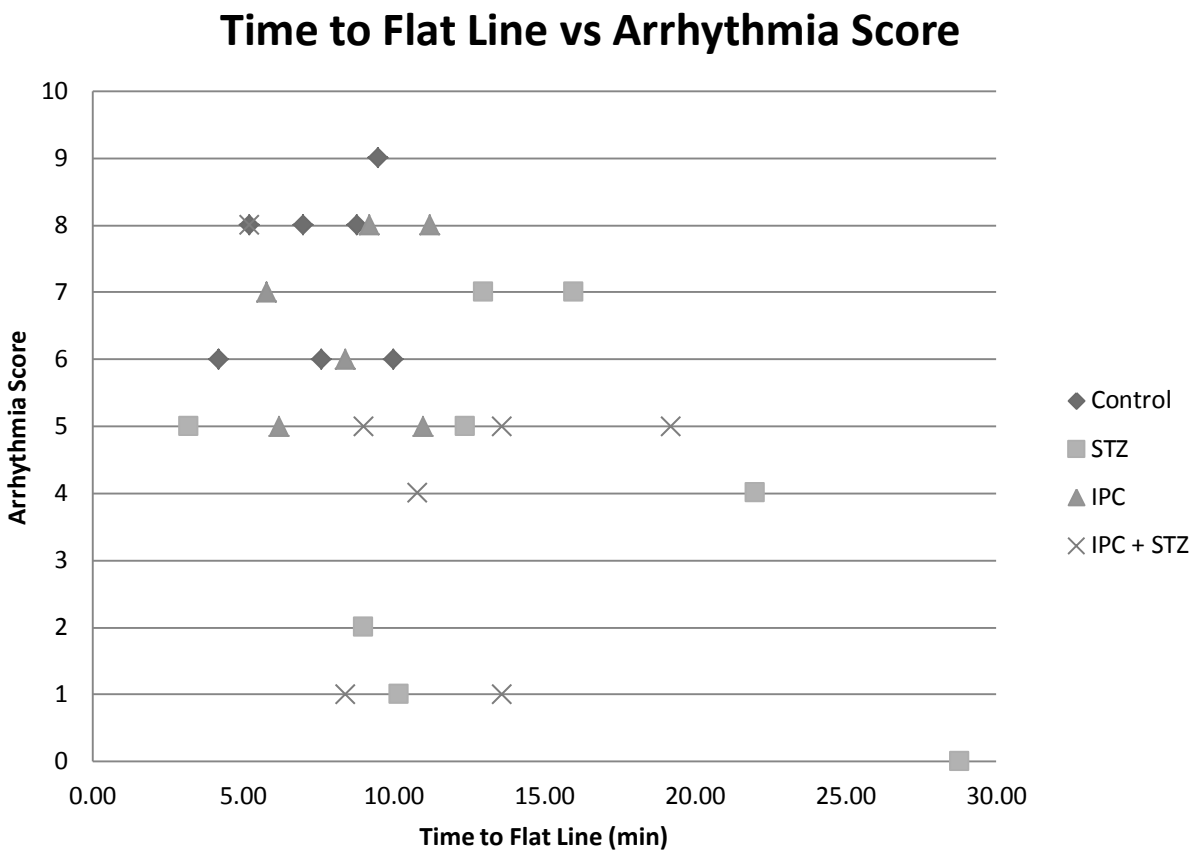

Figure 26 Lack of correlation between time to flat line and arrhythmia scores for individual animals. Control n=7, STZ n=7, IPC n=6 and IPC+STZ n=7.

The analysis of individual animals shows clearly that there is not a direct correlation between time to flatline and the arrhythmia score.

The arrhythmia scoring system depends on early sinus rhythm heavily. For this reason the ECG records were further analyzed in blocks of 10 minutes (Figure 27

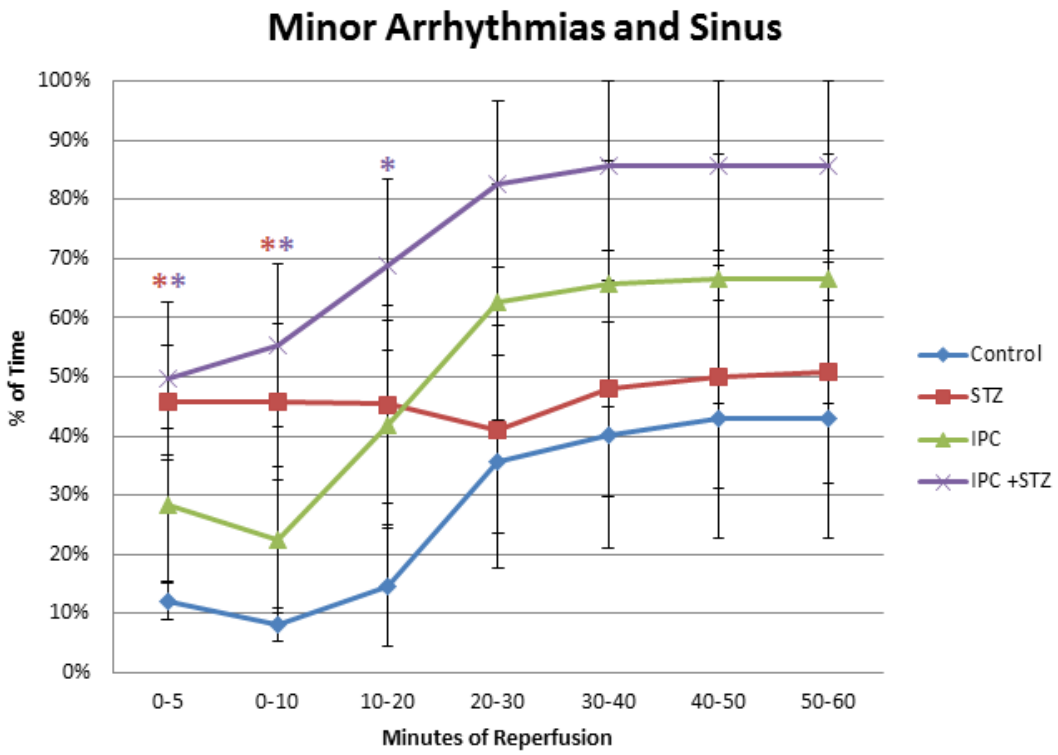

Figure **27**). Sinus rhythm and minor arrhythmias (ventricular premature beats and Bigeminy) were grouped together and the fraction of time spent in these conditions was recorded for each group.

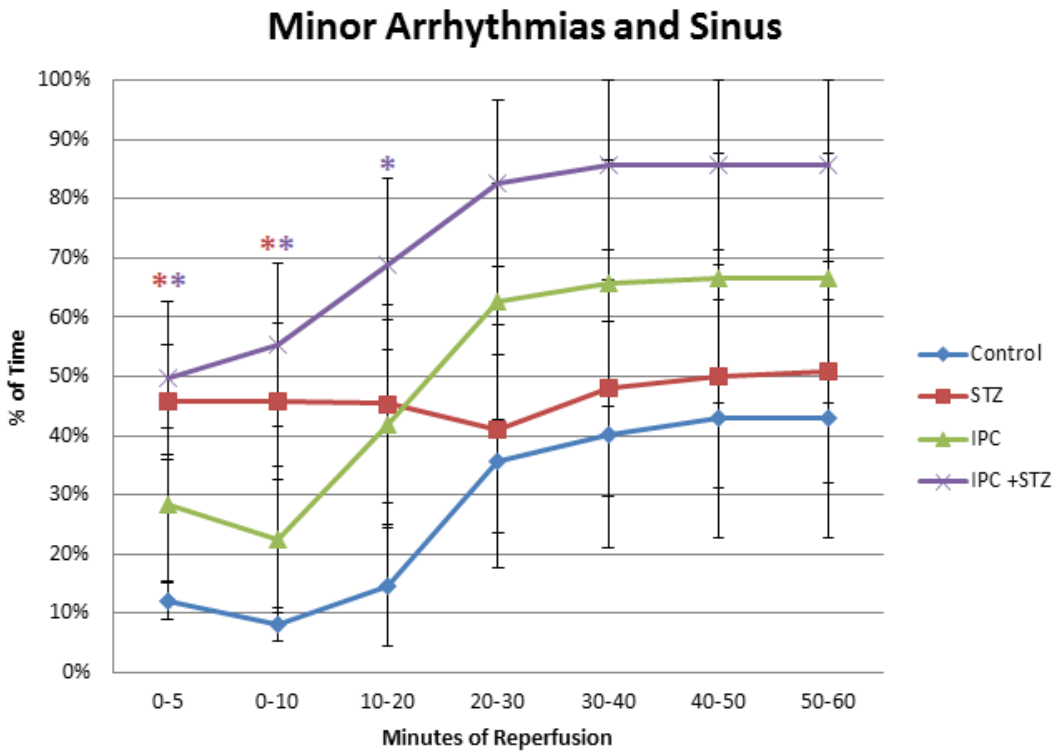

Figure 27 Time spent in minor arrhythmias or sinus rhythm. Minor arrhythmias include ventricular premature beats and Biheminy. * indicates $p < 0.05$ using two tailed t-test. Control n=8, STZ n=7, IPC n=6 and IPC+STZ n=7.

This break-down shows why STZ and STZ + IPC have such low arrhythmia scores; the arrhythmia scoring system gives highest scores for arrhythmias in the first minute of the reperfusion that do not reverse over the 60 minutes reperfusion. Therefore, control and IPC have the highest scores. STZ and STZ + IPC have much lower arrhythmia scores, owing to the high probability of sinus rhythm during early reperfusion (the first 5 minutes). IPC has a high likelihood of naturally reverting to sinus rhythm after about 20 minutes, resulting in healthier ECG's after 60 minutes reperfusion than STZ animals (not statistically significant). IPC + STZ

fares best, combining the starting advantage of STZ's high sinus rate and the increase in sinus rate of IPC around 20 minutes.

The benefits in terms of arrhythmia risk of IPC and STZ appear to work on different time scales. Subjects within a group also diverge with time, making statistical significance more difficult to achieve.

3.3 Experiment 2 Activation Time Response to Ischemia:

Activation times were determined for STZ and control animals during the IPC protocol to determine whether STZ had any effect on conduction during the IPC protocol (Figure 28).

There was no significant difference between control and STZ animals during the IPC protocol as shown in Figure 29.

In Figure 29 the activation times during the final 10 minutes ischemia were determined and normalized to control recording. Due to many subjects flat lining or entering fibrillation prior to 10 minutes of ischemia only the first 5 minutes of ischemia were evaluated.

Activation times for STZ and IPC are similar at 2 minutes ischemia. However, activation times are more prolonged in IPC at 5 minutes, which is statistically different from STZ. IPC + STZ is between IPC and STZ groups at 5 minutes though not statistically different from either.

Normalized activation time over the first 5 minutes of ischemia were further broken down minute by minute in Figure 30.

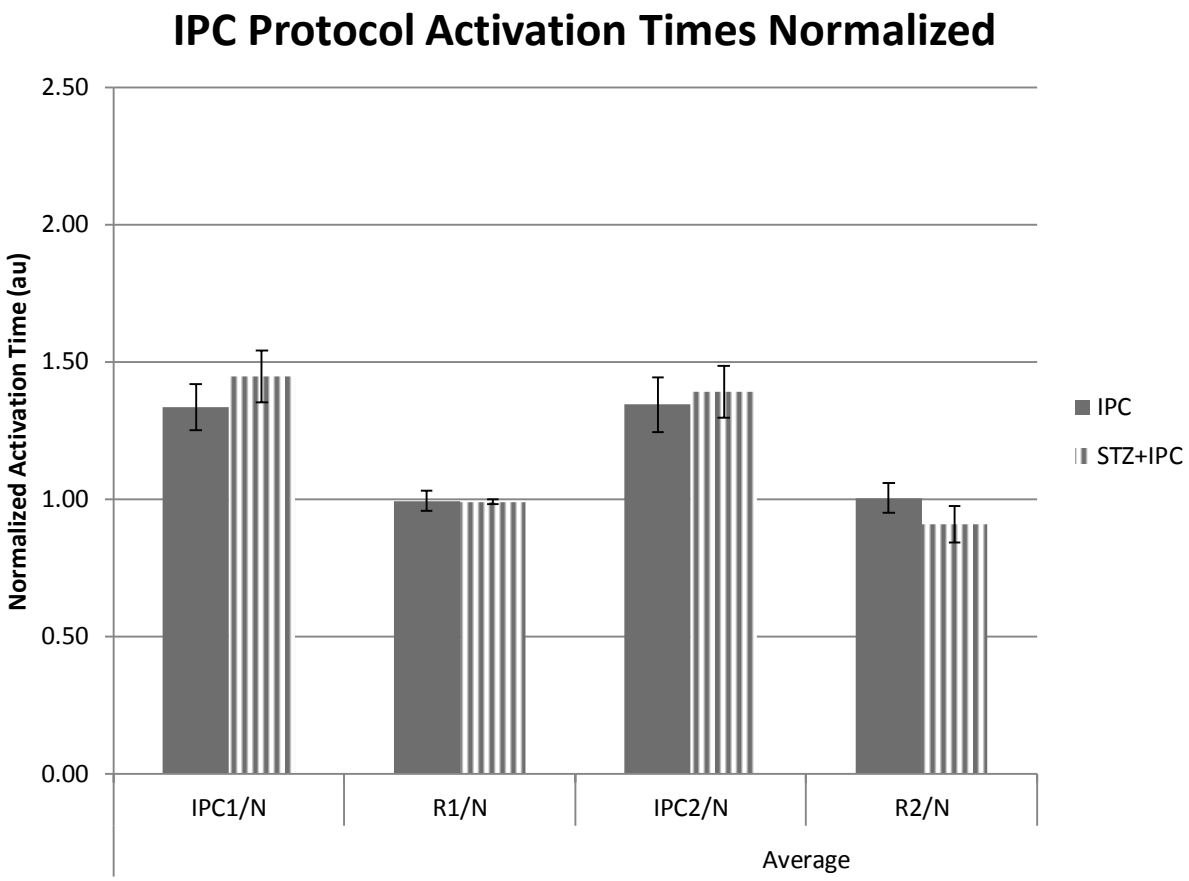

Figure 28 Activation times of tissue (normalized to recording taken before IPC protocol) for IPC protocol. IPC1/N is the normalized conduction velocity after the first period of ischemia, R1/N after the first reperfusion, IPC/N after the second ischemia and R2/N after the final ischemia. IPC n=6 STZ+IPC n=4.

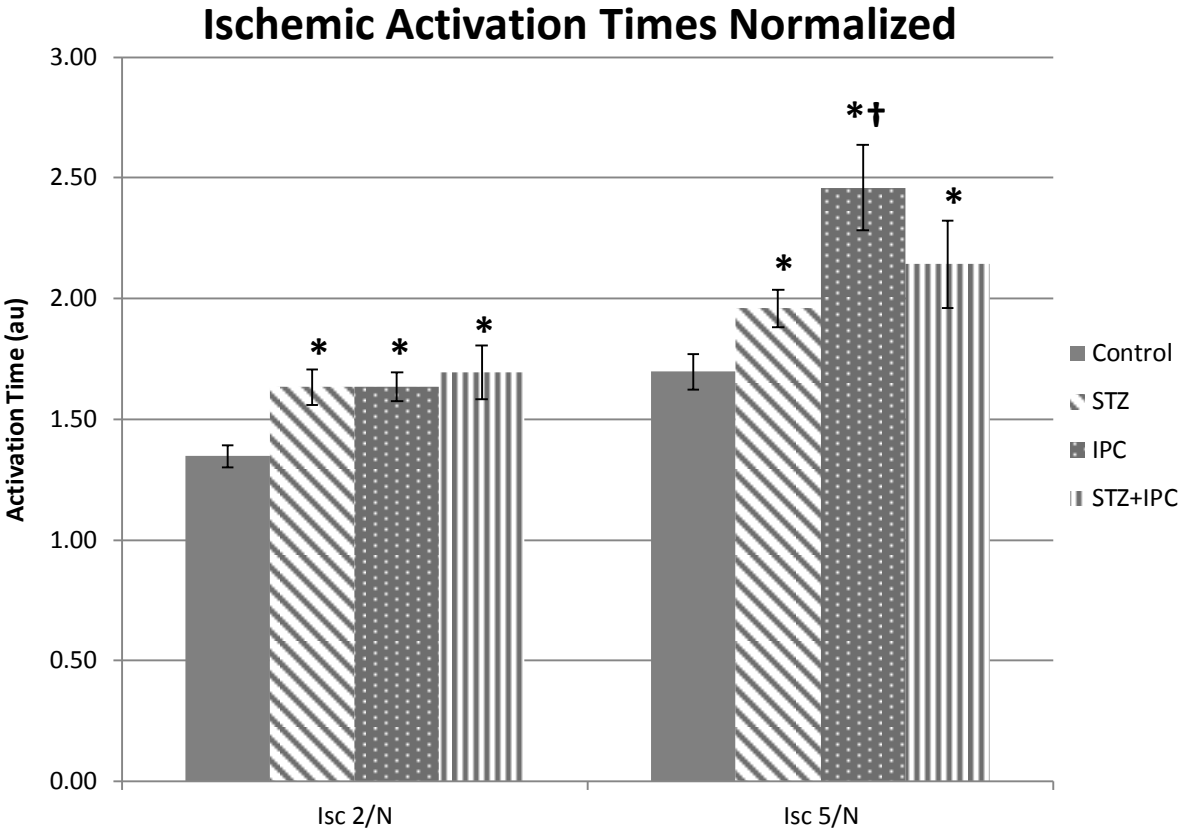

Figure 29 Activation Times during final ischemia. * indicates a significant difference ($p < 0.05$) with respect to Control, † indicates $p < 0.05$ with respect to STZ. Dunn's Piecewise Method was used. Control n=7, STZ n=8, IPC n=10 and STZ+IPC n=9.

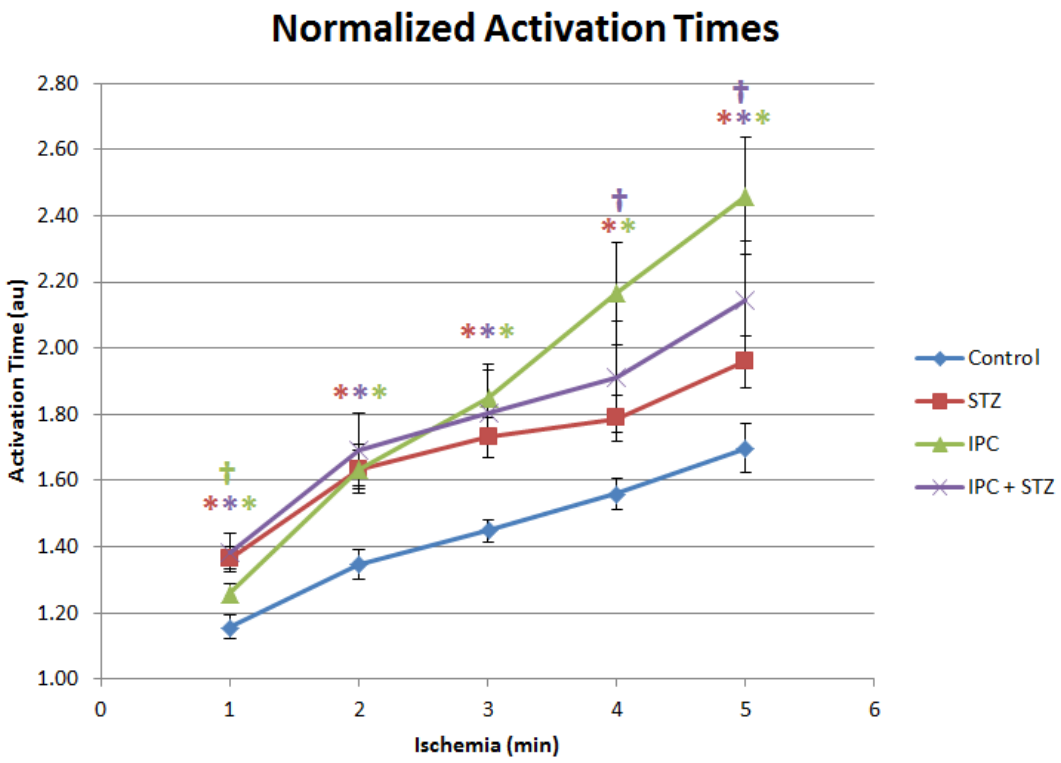

Figure 30 Normalized Activation Times for first 5 minutes of ischemia. * indicates $p < 0.05$ with respect to Control, † indicates $p < 0.05$ with respect to STZ. Dunn's Piecewise Method was used.

These results show that IPC has a faster activation time initially to ischemia compared to STZ. However, the rate of slowing of conduction in response to ischemia is much greater. IPC + STZ shows an average of the STZ and IPC behavior.

The rate of slowing for the tissue activation time is shown in Table 5 for each group. The STZ slowing is similar to that of the control group, suggesting that differences between STZ and control are due to initial starting conditions. The difference in rate of slowing between STZ and IPC indicate different mechanism and the averaging effect in IPC + STZ (though not significant) indicates competing mechanisms.

Table 5 p values for statistical differences of rates of slowing for normalized activation times from IPC data. (1 to 5 minute periods, significant values $p<0.05$ are bolded.

	Rate of Change in Slowing TTEST				
	1 to 2 min	2 to 3 min	3 to 4 min	4 to 5 min	1 to 5 min
Control vs STZ + IPC	0.218	0.971	0.510	0.044	0.227
Control vs IPC	**0.022**	**0.022**	0.080	0.112	**0.008**
Control vs STZ	0.251	0.915	0.284	0.565	0.711
IPC + STZ vs IPC	0.629	**0.026**	0.142	0.848	0.084
STZ vs IPC	0.245	**0.023**	**0.031**	0.192	**0.011**
STZ vs STZ + IPC	0.657	0.909	0.085	0.108	0.295

3.4 Experiment 3 Effect of IPC and STZ on Conduction Reserve

The increase in activation time, a measure of the slowing of the wave front, in response to high extracellular K^+ is shown in Figure 31. Tissue with a lower number of functional gap junctions results in a reduced conduction reserve.

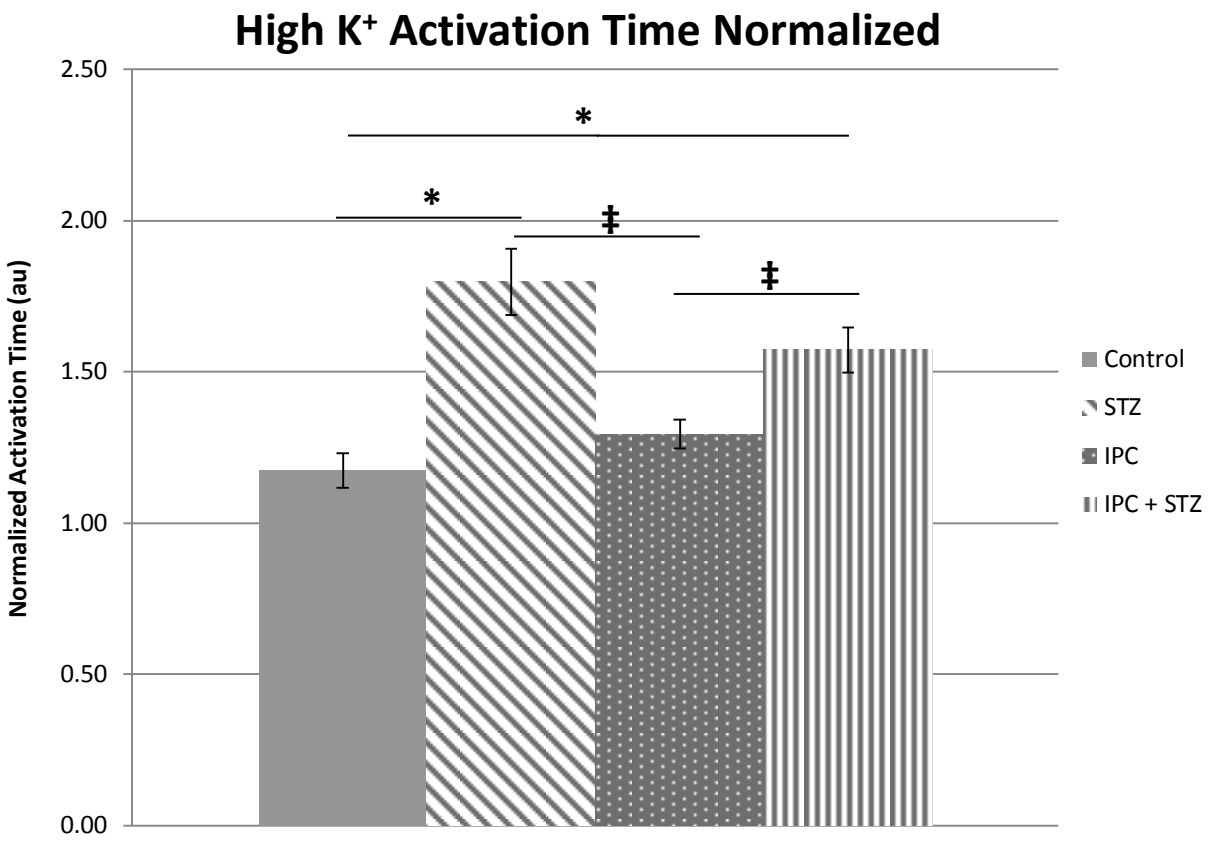

Figure 31 Activation times of tissue after being exposed to 9mM K^+ K-H buffer for 10 minutes. * indicates significant difference ($p < 0.05$) to control and ‡ indicated significant difference to IPC using One Way ANOVA. Control n=8, STZ n=10, IPC n=11 and IPC+STZ n=12.

IPC behaves similarly to control (no significant difference), while conduction slowing in both STZ and IPC + STZ is significantly more pronounced than in IPC and Control. IPC + STZ shows an average response between IPC and STZ groups, though the difference between STZ and STZ + IPC only has a p value of 0.109 (not statistically significant).

Chapter 4 Discussion

4.1 Hypothesis 1) STZ hearts and healthy control hearts subjected to IPC have similar frequency of ischemia-reperfusion arrhythmias

By clearly demonstrating a difference in frequencies of STZ and control ischemia reperfusion (IR) arrhythmias after IPC treatment the results did not prove Hypothesis 1.

The STZ group had the greatest anti-arrhythmic effects as expected by previous work [8]. Zang, et al. (2002) evaluated arrhythmias by the percentage of animals to display VT, sustained VT, VF or sustained VF during the first 30 minutes of reperfusion. Figure 27 from section 4.2 illustrates our research corresponds with Zang, et al. (2002) results. Control tissue has a low percentage of sinus rhythm in the first 20 minutes of reperfusion. This would result in a poor arrhythmia evaluation by Zang; similarly has a STZ has a high early reperfusion percentage in sinus rhythm resulting in a lower arrhythmia score.

The STZ and IPC + STZ groups in this work received a low arrhythmia score from the arrhythmia scoring system's strict scoring for early arrhythmias [45]. The IPC tissue had a better rate of sinus rhythm after approximately 20 minutes of reperfusion which may mean it provides a better long term response to ischemia than diabetes. IPC animals did fare better from ischemia/reperfusion, as expected from literature [7], however not on the same time scale as STZ. Alsaddique (2000) indicates that IPC's cardio protective effects come from a reduction in myocardial death due the ischemia; this conclusion may indicate the cause for the findings in our work regarding IPC following the same profile as control tissue (with respect to time scale). IPC

starts off with a greater percentage sinus rhythm and that advantage is maintained over control tissue throughout 60 minutes reperfusion.

While the arrhythmia scores appeared lowest in groups with the longest time to flat line, the time to flat line and arrhythmia score were compared for correlation in each animal. This analysis clearly illustrated that there is no direct correlation between time to flat line and arrhythmia score for re-perfused tissue. No similar comparison was found in the literature. However, the heart rate slowing seen during ischemia may result in a greater supply of ATP upon reperfusion allowing sinus rhythm to return immediately in STZ hearts. IPC, which does not have a slowing of heart rate, takes longer (as does control to a lesser extent) to return to sinus rhythm. This may be due to the need for ATP to build up to a healthy level for sustained sinus rhythm. This theory would also support why tissue does not substantially increase (for STZ hearts) the number of hearts in sinus over time while it does for IPC and control. STZ specimens do not need to "build up" ATP to a healthy level during reperfusion, and therefore there is no time dependent response. The STZ tissue is either able to sustain sinus rhythm or not upon reperfusion.

IPC behaves similarly to control during reperfusion (also seen during R-R Interval, and high K^+ experiments) however IPC begins reperfusion with greater rate of sinus rhythm. This corresponds to work showing IPC is an effective method for increasing glucose uptake during reperfusion after long periods of ischemia [46].The benefits of IPC are therefore starting at reperfusion, and that IPC does not stop the return to sinus rhythm after 20 minutes reperfusion (which STZ does).

STZ does not show any changes in sinus rhythm over time; our IPC + STZ group did not display the same time dependent behavior as STZ. This effect cannot be attributed to STZ induced cell death caused by the MPTP as STZ has been shown to override IPC to activate the MPTP [40].

4.2 Hypothesis 2) STZ hearts and healthy control hearts subjected to IPC have similar reductions of conduction reserve.

Due to contradictory results from Experiments 1, 2, and 3 the similarities between STZ and IPC cannot be determined.

As Ghaly 2009 illustrated, lateralization of gap junctions leads to a decreased conduction reserve. Both IPC and STZ showed a significant decrease in conduction reserve compared to healthy controls as expected during paced ischemia (illustrated Experiment 2). These results can be connected to the gap junction dysfunction seen in both STZ and IPC animals [4], [10].

IPC did not show the expected reduction in conduction reserve during high K^+ experiments. The paced tissue's response to ischemia mimics that of the non-paced, in that the conduction velocity of the tissue slows. IPC has been shown to induce gap junction lateralization [3] which may correlate to slowing of conduction velocity during ischemia, however IPC showed no significantly different response to high extracellular K^+ in Experiment 3, indicating gap junction lateralization either had not significantly occurred during IPC or that gap junctions alone are not responsible for conduction velocity slowing. IPC has been shown to have an immediate effect on gap junction conductance [47], resulting in similar electrical impedance on gap junction conductance to that of diabetes. However, IPC has different effect on electrical impedance of gap junction communication to that of chemical impedance of gap junction communication which

has a delayed onset during ischemia [47]. High K^+ may not have the slowing effect of ischemia on IPC tissue due to the discrepancy of IPC effects on Connexin 43 between electrical and chemical coupling of cells.

A 3 minute period of ischemia for IPC was selected because a 5 minute period resulted in many subjects not surviving the IPC procedure. Naitoh et al, (2009) performed an IPC protocol of 2 repeated intervals of 5 minutes of ischemia followed by 5 minutes reperfusion. Our IPC protocol may not have been long enough for significant gap junction lateralization without the final ischemia. The rate of slowing for the conduction velocity is greater than its control equivalent. This indicates a physiological change from control tissue; if gap junction lateralization continues throughout ischemia then the rate of slowing would be expected to increase as seen in this data.

A second explanation for the ineffectiveness of high K^+ to elicit a significant slowing of conduction velocity is that loss of gap junction functionality is insufficient to explain tissue response to reduced tissue excitability. Ghaly et al, (2009) provided a simulation which indicated that gap junction lateralization cannot account for all of the exaggerated response to high K^+ seen in STZ hearts. However, even with this consideration High K^+ would be expected to have a significant or near significant effect on tissue with lateralized gap junctions as it decreases cell excitability, stressing the tissue's conduction reserve. Therefore while previous work can explain potential differences between diabetic and IPC animals it cannot explain the inability of High K^+ not generating a significant difference in response between IPC and Control.

STZ differed from control in slowing of conduction velocity to control during ischemia, which is expected with a lower conduction reserve. This response was observed during paced ischemia in the first 5 minutes. As high extracellular K^+ decreases the excitability of myocardial tissue [47] the gap junctions between cells are critical for conduction propagation through tissue. Simulated STZ had a decrease in the number of functional gap junctions which exaggerates the tissues response to high extracellular K^+ compared to healthy control tissue [21]. Further the rate of slowing of the conduction velocity is very similar to that of control, indicating that the initial differences between control and STZ are responsible for the significant differences in response to ischemia. This early difference from control may be correlated to the decreased number of functional gap junctions and the increased sensitivity to high extracellular K^+.

STZ and IPC animals were different in response to high extracellular K^+ and during non-paced ischemia indicating a difference gap junction lateralization time scale or a secondary competing mechanism.

4.3 Hypothesis 3) IPC does not further reduce conduction reserve or frequency of ischemia-reperfusion arrhythmias in STZ hearts.

STZ and IPC have not been directly compared for their effects on conduction reserve before this study. As Hypothesis 1 was not proven and Hypothesis 2 could not be substantiated, IPC and STZ cannot be assumed to be using the same mechanism for cardio protection.

IPC + STZ tissue repeatedly displays results that are an “average” of IPC and STZ animals. This averaging indicates two competing mechanisms within IPC and STZ. If the mechanisms were

simply unrelated then IPC + STZ would be expected to behave as either IPC or STZ depending on the experiment; however, this is not the case.

A second explanation for the "averaging" effect of the IPC + STZ group could be that STZ provides some protective mechanism for the tissue so IPC does not need to take full effect. However during reperfusion IPC + STZ tissue increases the sinus rhythm after 20 minutes which was also seen in both IPC and control. As STZ does not have this behavior the addition of the IPC protocol appears to cause the tissue to revert back to the control behavior. This additive protection disproves Hypothesis 3.

These differences cannot be attributed to the effect IPC has on the MPTP. IPC and STZ both activate iPLA2 increasing Ca^{2+} release which would lead to MPTP opening and cell death, however in IPC a second pathway is opened which suppresses the MPTP from opening. STZ overrides IPC [40], forcing the MPTP open. Therefore if the MPTP was responsible for the anti-arrhythmic protection of IPC, the IPC + STZ group would be expected to have a worse outcome during reperfusion (which was not the case).

4.4 Differences and Similarities Between IPC and STZ

STZ and IPC have a number of distinct physiological differences which is repeatedly demonstrated in this work. In Figure 22, STZ has a slowing of heart rate in response to ischemia (and a slower initial heart rate) while IPC has a lower initial heart rate and similar slowing of heart rate to control hearts.

The inverse is seen for slowing of conduction velocity during ischemia (Figure 24), where STZ has a similar slowing to control tissue while IPC conduction velocity slows significantly. During paced ischemia (Figure 30) both STZ and IPC show slowing of conduction velocity. This indicates that in an unpaced situation STZ does not show signs of conduction slowing in the first 5 minutes as heart rate slowing is sufficient or extracellular potassium has not yet built up to decrease the excitability of the cells which would exaggerate conduction velocity slowing due to decrease in number of functional gap junctions.

Arachidonic acid (AA) may also play a role. Both IPC and STZ are shown to increase iPLA2 activation which produces AA's [35]. AA's alter the myocardial physiology resulting in slowing of conduction velocity and lengthening of the action potential.

IPC has a higher rate of slowing during ischemia than STZ tissue (Figure 22); this may be due to the theory that IPC begins lateralization of gap junctions during prolonged ischemia while STZ has already lateralized its gap junctions. The difference in response to high extracellular K^+ (Figure 31) can also be explained by this theory. STZ with already lateralized gap junctions is more sensitive to high K^+ while IPC does not lateralize it's gap junctions as there is no prolonged ischemia to induce lateralization and thus behaves more similarly to control tissue.

Chapter 5 Conclusions and Recommendations

The goal of this work was to show that the metabolic similarities between diabetes and IPC shown in the literature correlate to similar whole heart anti-arrhythmic effects. However this work indicates that diabetes and IPC do not have a similar whole system effects with respect to ischemia reperfusion arrhythmias.

Diabetes induced by STZ and ischemic preconditioning are not functioning on the same time scale and therefore are not equivalently activating protective anti-arrhythmic mechanisms. Further STZ and IPC appear to activate competing mechanisms when both are embodied in the same tissue (IPC + STZ). While both IPC and STZ do display a decrease in conduction reserve their responses to non-paced ischemia are significantly different, indicating different mechanism for dealing with ischemia.

More work should be done to determine which protective anti-arrhythmic mechanism is more beneficial; diabetes' high initial sinus rhythm during reperfusion, or IPC's late onset increase of sinus rhythm after 20 minutes with a marginally greater initial sinus rhythm than control tissue. As STZ and IPC did appear to be additive for anti-arrhythmia effects, it would be ideal to learn to activate both mechanisms simultaneously.

A study into the effect of heart rate on STZ and IPC response to ischemia should be considered. In this work, STZ had a slowing of heart rate during ischemia, however during pacing it behaved similarly to IPC. STZ and IPC should be compared during ischemia with sinus node pacing to

determine if STZ slows both its heart rate and conduction velocity in response to non-paced ischemia.

Hypothesis 2 should be further evaluated, attempting a stronger IPC protocol with longer periods of ischemia. Another study should be done to determine the effect of high initial levels of ATP at reperfusion onset have on ischemia reperfusion arrhythmias. Work should be done to determine the metabolic significance of ischemia on IPC for cardio protection in ischemia reperfusion arrhythmias. Metabolic changes during final ischemia may explain why IPC conduction velocity slows during ischemia but not during high extracellular K^+.

This work was a macroscopic, whole heart study to compare the cardio protective effects of IPC and diabetes with respect to ischemia reperfusion arrhythmias. This work shows that while literature points to a number of metabolic similarities the whole heart protective effect for the two are not comparable. They operate on different time scales, and IPC may require final ischemia to fully activate its protective mechanism.

References

[1] Iltis, Kober, Dalmasso, Cozzone and Bernard, "Noninvasive characterization of myocardial blood flow in diabetic, hypertensive, and diabetic-hypertensive rats using spin-labeling MRI," *Microcirculation,* pp. 607-14, 2005.

[2] Fein, "Diabetic cardiomyopathy," *Diabetes Care,* pp. 1169-79, 1990.

[3] Naitoh, Yano, Miura, Itoh, Miki, Tanno, Sato, Hotta, Terashima and Shimamoto, "Roles of Cx43-associated protein kinases in suppression of gap junction-mediated chemical coupling by ischemic preconditioning," *Am J Physiol Heart Circ Physiol,* pp. H396-H403, 2009.

[4] Nygren, Olson, Chen, Emmett, Kargacin and Shimoni, "Propagation of the cardiac impulse in the diabetic rat heart: reduced conduction reserve," *J Physiology,* pp. 543-60, 2007.

[5] Rahnema, Shimoni and Nygren, "Reduced conduction reserve in the diabetic rat heart: role of iPLA2 activation in the response to ischemia," *Am J Physiol Heart Circ Physiol,* p. H326–H334, 2011.

[6] Williams and Gottlieb, "Inhibition of mitochondrial calcium-independent phospholipase A2 (iPLA2) attenuates mitochondrial phospholipid loss and is cardioprotective.," *Biochem J,* pp. 23-32, 2002.

[7] Alsaddique, "Ischemic Preconditioning: The Endogenous Power A Review of the Literature," *Angiology,* pp. 355-360, 2000.

[8] Zhang, Parratt, Beastall, Pyne and Furman, "Streptozotocin diabetes protects against arrhythmias in rat isolated hearts: role of hypothyroidism," *European Journal of*

Pharmacology, pp. 269-276, 2002.

[9] Ovize, Aupetit, Rioufol, Loufoua, Andre-Fouet, Minaire and Faucon, "Preconditioning reduces infarct size but accelerates time to ventricular fibrillation in ischemic pig heart," *Am J Physiol Heart Circ,* pp. H72-H79, 1995.

[10] Severs, Bruce, Dupont and Rothery, "Remodelling of gap junctions and connexin expression in diseased myocardium," *Cardiovasc Res,* pp. 9-19, 2008.

[11] Mohrman and Heller, Cardiovascular Physiology, McGraw Hill, 2006.

[12] Fraser, Harley and Wiley, "Electrocardiogram in the normal rat.," *Journal of Applied Physiology,* pp. 23:401-402, 1967.

[13] Sohl and Willecke, "Gap Junctions and the Connexin Protien Family," *Cardiovascular Research,* pp. 228-232, 2003.

[14] Verheijck, v. Kempen, Analbers and Gros, "Spatial distribution of connexin43, the major cardiac gap junction protein, visualizes the cellular network for impulse propagation from sinoatrial node to atrium.," *Circ Res,* pp. 802-11, 1995.

[15] Okruhlicova, Tribulova, Misejkova, Kucka, Stetka and Slezak, "Gap junction remodelling is involved in the susceptibility of diabetic rats to hypokalemia-induced ventricular fibrillation," *Acta Histochem,* pp. 387-91, 2002.

[16] Stein, v. Veen, Remme, Boulaksil, Moorman, Stuijvenberg, v. d. Nagel, Bezzina, Hauer, Bakker and v. Rijen, "Combined reduction of intercellular coupling and membrane excitability differentially affects transverse and longitudinal cardiac conduction," vol. 83, no. 1: 52-60, 2009.

[17] Mines, "On dynamic equilibrium in the heart," *J Physiol,* pp. 349-83, 1913.

[18] Kleber and Rudy, "Basic mechanisms of cardiac impulse propagation and associated arrhythmias," *Physiol Rev,* pp. 431-88, 2004.

[19] S. R. Rudy Y, "Cardiac excitation: an interactive process of ion channels and gap junctions," *Adv Exp Med Biol,* pp. 269-79, 1997.

[20] Ghaly, Boyle, Vigmond, Shimoni and Nugren, "Simulations of reduced conduction reserve in the diabetic rat heart: response to uncoupling and reduced excitability," *AnnBiomed Eng,* pp. 1415-25, 2010.

[21] Ghaly, Boyle, Vigmond, Shimoni and Nygren, "Simulations of Reduced Conduction Reserve in Diabetic Rat Heart Resonse to Uncoupling and Reeduced Excitability," *Annals of Biomedical Engineering,* pp. 1414-1425, 2009.

[22] Thrainsdottir, Aspelund, Thorgeirsson, Gudnason, Hardarson and Malmberg, "The association between glucose abnormalities and heart failure in the population-based Reykjavik study," *Diabetes Care,* pp. 612-616, 2005.

[23] Bertoni, Hundley, Massing, Bonds, Burke and Goff, "Heart failure prevalence, incidence, and mortality in the elderly with diabetes," *Diabetes Care,* pp. 699-703, 2004.

[24] Mak, Moliterno, Granger, Miller, White and Wilcox, "Influence of diabetes mellitus on clinical outcome in the thrombolytic era of acute myocardial infarction. GUSTO-I Investigators. Global Utilization of Streptokinase and Tissue Plasminogen Activator for Occluded Coronary Arteries.," *J Am Coll Cardiol,* pp. 171-179, 1997.

[25] Mayama, Matsumura, Lin, Ogawa and Imanaga, "Remodelling of cardiac gap junction

connexin 43 and arrhythmogenesis," *Exp Clin Cardiol,* pp. 67-76, 2007.

[26] Lin, Ogawa, Imanaga and Tribulova, "Remodeling of connexin 43 in the diabetic rat heart," *Mol Cell Biochem,* pp. 69-78, 2006.

[27] Yin, Zheng, Zhai, Zhao and Cai, "Diabetic Inhibition of Preconditioning- and Postconditioning-Mediated Myocardial Protection against Ischemia/Reperfusion Injury," *Experimental Diabetes Research,* p. Article ID 198048, 2012.

[28] Jain, Schuessler and Saffitz, "Mechanisms of Delayed Electrical Uncoupling Induced by Ischemic Preconditioning," *Circulation Research,* p. 1138, 2003.

[29] Schulz and Heusch, "Connexin 43 and ischemic preconditioning," *Cardiovascular Research,* pp. 335-344, 2004.

[30] Poitout and Robertson, "Minireview: Secondary β-Cell Failure in Type 2 Diabetes—A Convergence of Glucotoxicity and Lipotoxicity," *Endocrinology,* p. 339, 2002.

[31] Görbe, Varga, Kupai, Bencsik, Kocsis, Csont, Boengler, Schulz and Ferdinandy, "Cholesterol-diet leads to attenuation of ischemic preconditioning-induced cardiac protection: the role of connexin43," *Am J Physiol Heart Circ Physiol,* pp. H1907-H1913, 2011.

[32] Galagudza, Syrensky and Alexandrov, "Ischemic preconditioning and myocardial tolerance to ischemia in," *DAVID KOPF INSTRUMENTS,* p. Kopf Carrier #70, 2010.

[33] McHowat and Creer, "Catalytic features, regulation and function of myocardial phospholipase A2," *Curr Med Cardiovasc Hematol Agent,* pp. 209-18, 2004.

[34] Cedars, Jenkins, Mancuso and Gross, "Calcium-independent phospholipases in the heart: mediators of cellular signaling, bioenergetics, and ischemia-induced electrophysiologic

dysfunction," *J Cardiovasc Pharmacol,* pp. 277-89, 2009.

[35] V. V. W. M. W. R. Schmilinsky-Fluri G, "Modulation of cardiac gap junctions: the mode of action of arachidonic acid," *J Mol Cell Cardiol,* pp. 1703-13, 1997.

[36] Naserabad, "Cardiac Impulse Propagation in Diabetic Heart: Response to Oxidative Stress and Ischemia," 2011.

[37] Smani, Zakharov, Leno, Csutora, Trepakova and Bolotina, "Ca2-independant Phospholipase A2 Is a Novel Determinant of Store-operated Ca2 Entry," *Journal of Biological Chemistry,* pp. 11909-11915, 2003.

[38] Kersten, Toller, Gross, Pagel and Warltier, "Diabetes abolishes ischemic preconditioning: role of glucose, insulin, and osmolality," *AJP - Heart,* pp. H1218-H1224, 2000.

[39] Juhaszova, Zorov, Kim, Pepe, Fu, Fishbein, Ziman, Ytrehus, Antos, Olson and Sollott, "Glycogen synthase kinase-3β mediates convergence of protection signaling to inhibit the mitochondrial permeability transition pore," *Journal of Clinical Investigation,* p. 1535–1549, 2004.

[40] Yadav, Singh and Sharma, "Involvement of GSK-3b in attenuation of the cardioprotective," *Mol Cell Biochem,* pp. 75-81, 2010.

[41] Nygren, Kondo, Clark and Giles, "Voltage-sensitive dye mapping in Langendorff-perfused rat hearts," *Am J Physiol Heart Circ Physiol,* pp. H892-H902, 2003.

[42] Larsen, Sciuto, Moreno and Poelzing, "The voltage-sensitive dye di-4-ANEPPS slows conduction velocity in isolated guinea pig hearts," *Article in Press,* 2012.

[43] LeGrice, Smaill, Chai, Edgar, Gavin and Hunter, "Laminar structure of the heart: ventricular

myocyte arrangement and connective tissue architecture in the dog," *Am J Physiol Heart Circ Physiol,* pp. 269:H571-H582, 1995.

[44] Walker, Curtis, Hearse, Cambell, Janse, Yellon, Cobbe, Coker, Harness, Harron and Higgins, "The Lambeth Conventions: guidelines for the study," *Cardiovascular Research,* pp. 447-455, 1988.

[45] Curtis and Walker, "Quantification of arrhythmias using scoring systems: an examination of seven scores in an in vivo model of regional myocardial ischaemia," *Cardiovascular Research,* pp. 656-665, 1988.

[46] Fischer-Rasokat, Beyersdorf and Doenst, "Insulin addition after ischemia improves recovery of function equal to ischemic preconditioning in rat heart," *Basic Research in Cardiology,* pp. 329-336, 2003.

[47] Miura, Miki and Yano, "Role of the gap junction in ischemic preconditioning in the heart," *American Journal of Physiology - Heart and Circulatory Physiology,* vol. 298, pp. H1115-H1125, 2010.

[48] Gettes and Surawicz, "Effects of low and high concentrations of potassium on the simultaneously recorded Purkinje and ventricular action potentials of the perfused pig moderator band," 1968.

[49] Crompton, "The mitochondrial permeability transition pore and its role in cell death," *Biochem K,* pp. 233-249, 1999.

[50] Howarth, Nowotny, Zilahi, Haj and Lei, "Altered expression of gap junction connexin proteins may partly underlie heart rhythm disturbances in the streptozotocin-induced

diabetic rat heart," *Mol Cell Biochem,* p. 145–151, 2007.

[51] Murc, Almeida, Raizada and Ferreira, "Chronic activation of endogenous angiotensin-converting enzyme 2 protects diabetic rats from cardiovascular autonomic dysfunction," *Exp Physiol,* pp. 699-709, 2012.

[52] Shimoni, Emmett, Schmidt, Nygren and Kargacin, "Sex-dependent impairment of cardiac action potential conduction in type 1 diabetic rats," *Heart and Circulatory Physiology,* p. H1442–H1450, 2009.

[53] Hausenloy, Tsang, .. Mocanu and Yellon, "Ischemic preconditioning protects by activating prosurvival kinases at reperfusion," *Am J Physiol Heart Circ Physiol,* pp. 288:H971-H976, 2005.

[54] Stein and V. Veen, "Combined reduction of intercellular coupling and membrane excitability differentially affects transverse and longitudinal cardiac conduction," no. 52-60 , 52-60 .

Appendix A Data Collection and Processing

Table A1: Experiment Number and corresponding raw data collection and data processing.

Experiment Number	Group	Number of Animals	Data Collected By	Data Processed By
1	Control	6	S Mishriki*	A Randall and S Mishriki**
		2	A Randall	A Randall
	STZ	6	S Mishriki*	A Randall and S Mishriki**
		2	A Randall	A Randall
	IPC	6	S Mishriki*	A Randall and S Mishriki**
	IPC + STZ	6	S Mishriki*	A Randall and S Mishriki**
		2	A Randall	A Randall
2	Control	7	P Rahnema	A Randall
	STZ	8	P Rahnema	A Randall
	IPC	10	A Randall	A Randall
	IPC + STZ	9	A Randall	A Randall
3	Control	8	Y Shimoni	A Randall
	STZ	10	Y Shimoni	A Randall
	IPC	11	A Randall	A Randall
	IPC + STZ	12	A Randall	A Randall

*S Mishriki collected data under the direct supervision by A Randall

**S Mishriki processed data on Time to Flat Line during final ischemia and categorization of arrhythmias during 60 minutes of reperfusion.